UNIVERSITY OF COPENHAGEN
FACULTY OF SCIENCE
NIELS BOHR INSTITUTE

Master of Science in Physics

Solving the turbulence closure problem II

Determining the deep ocean stratification

Rasmus Ranum Hansen

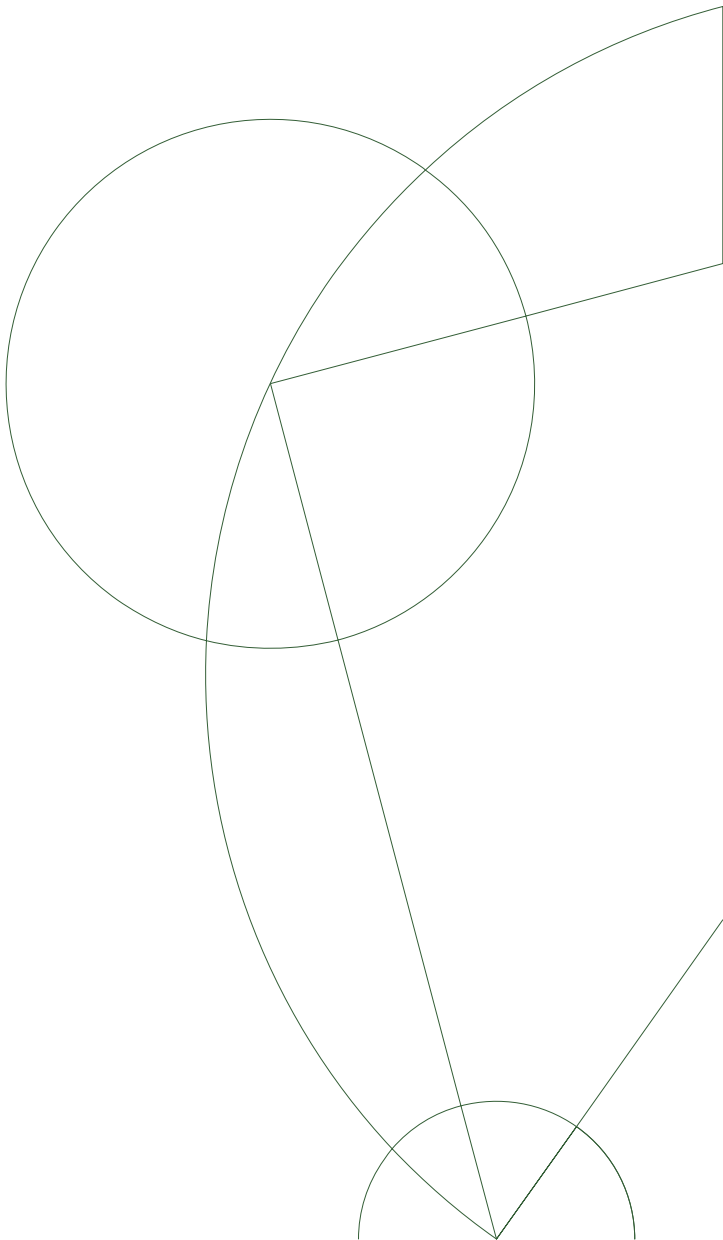

Supervisor
Markus Jochum

Handed in: May 20, 2023

ABSTRACT

This thesis aims to formalize the stratification of the deep ocean as a function of buoyancy and wind forcing. With the use of the ocean only model VEROS the AMOC is analysed in a idealistic Atlantic ocean model. Firstly the conclusions from Greatbatch and Lu (2003) were used as a starting point, analysing the relation between the AMOC strength and the meridonal buoyancy gradient found in Bryan (1987). Contrary to their paper we do not find that the Stommel box model closure from Bryan (1987) does not hold for low horizontal friction, but instead find it to be a good fit. We also find the southern ocean wind forcing to be in a superposition with the buoyancy forcing.

We then found that the closure described in Brüggemann and Eden (2011) is a good 2.5 dimensional prognostic model for coarse resolution models, speeding up modeling time.

Finally using a new closure following closely the theory from Bryan (1987), however without the use the desperate approximation of changing the gradient in the thermal wind relation. We find this closure to be dynamically consistent with a clear theory behind all assumptions, and we find it to match the model data as well as the old closure. We therefore suggests this new closure as a better alternative.

CONTENTS

LIST OF FIGURES

LIST OF TABLES

ACRONYMS

AMOC Atlantic meridonal overturning circulation

THC Thermohaline circulation

NADW North Atlantic deep water

G&L Greatbatch and Lu

B&E Brüggemann and Eden

CFL Courant–Friedrichs–Lewy-criterion

Part I

INTRODUCTION

1

MOTIVATION

The worlds climate is an incredibly intricate and complex system, with many different processes and connections interacting and evolving. This makes the task of trying to understand and explain the climate systems incredibly hard. However the climate is one of the most important areas of science for humankind, and understanding the dynamics is therefore of a high level of importance.

One of the more important climate systems is the Atlantic meridional overturning circulation (AMOC), as it has an important role in the redistribution of heat on a global scale. The AMOC moves warm water from the tropics towards the northern polar regions, and also in turn, colder water towards the equator. Due to the scale of the AMOC, the redistribution of heat from equator to the northern hemisphere has a enormous effect on the climate in Europe and eastern north America. When comparing northern Europe's climate with locations of similar latitudes, one should compare the climate in the United Kingdom and Denmark, with that of Alaska of northern Canada. This difference in climate is due to the heat being transported by the Gulf stream, which is part of the AMOC.

Because of the Importance of the AMOC it would be of great interest to understand the dynamics driving the overturning and how one could describe it from measurable values.

2

GOAL

As stated the AMOC is highly important for the climate system, and we therefore wish to understand the dynamics driving the system. Now the processes describing the dynamics of the AMOC and the more general thermohaline circulation (THC) are more or less understood in general, however some parts are still uncertain, such as the tropical upwelling (and a walk-through will be done later), however the goal of this thesis is to make a connection between the AMOC and the ocean surface forcings. More precisely we wish to describe how the deep ocean stratification is controlled of the surface wind stresses and the buoyancy forcings. This is of high interest as this would allow estimations of the AMOC purely from atmospheric values, which are much easier to observe compared to anything in the deep ocean. We will in this project be looking at the Strength of the AMOC as the value describing the deep ocean stratification.

We therefore aim for a mathematical relation between the AMOC strength and the surface buoyancy forcings from salinity and temperature and the wind stress acting on the surface.

3

BACKGROUND

The AMOC is part of the general THC which is the global density driven circulation, we will focus on the AMOC and the Atlantic. The AMOC is density driven, meaning the water transport is forced by a density difference between the tropics and the poles. The heat from the sun is not evenly distributed over the planets surface, and there is therefore a surplus of heat in the tropics, which is carried towards the colder northern Atlantic, due to a difference in temperature and salinity, and therefore density. This difference comes from the down welling water in the polar regions. Here the water cools and the surface salinity decreases due the precipitation and ice. This leads to the fresh surface water from the tropics to get heavier, than the water below and it therefore sinks and creates North Atlantic deep water (NADW). The NADW cell then becomes the return flow, moving in the abyssal ocean back to the tropics. Here we now have a clear stratification of a deep heavy return flow and a warm fresh northward flow. We will not be discussing any zonal structure of the AMOC and will see it as a zonal average, where these two cells can be clearly seen.

There is however one problem. When the cold NADW reaches the tropics it is heavier than the warm surface layer, so there is no clear density difference to drive an up welling of the abyssal waters. Now there are different theories describing how the NADW reached the surface again to complete the system. Two very influential papers and theories regarding this problem is Stommel (1961) and Stommel and Arons (1959). Using the theory from

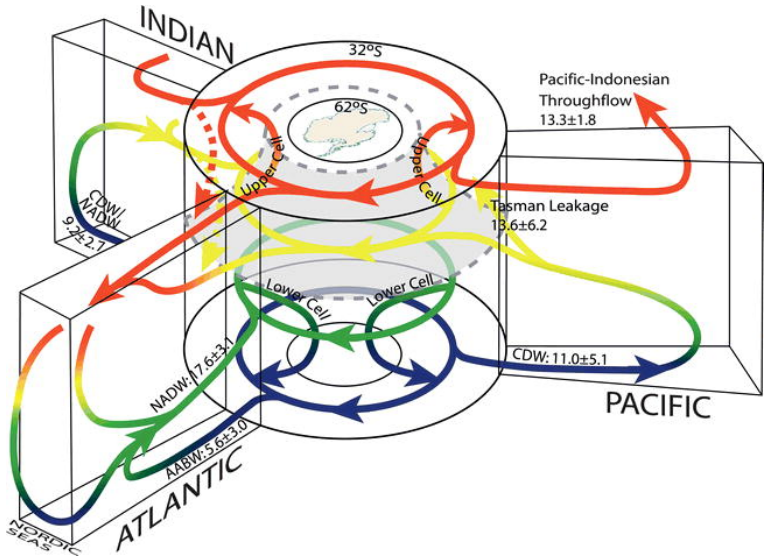

Figure 1: The Global Ocean Meridional Overturning cells without zonal structure, from *Lumpkin and Speer (2006)*

the Stommel paper Bryan (1987) derived a relation between the AMOC strength and the buoyancy forcings, which then describes what drives this up welling. However Straub (1996) showed that there is an inconsistency between the Stommel box model and the Stommel and Arons model, and the relation found in Bryan (1987) is therefore not dynamically consistent. We will now shed some light on both of these models and the dynamical inconsistency.

For both models we start with the Navier-Stokes equation, as they describe the motion in a viscous fluid:

$$\frac{\partial \vec{u}}{\partial t} + (\vec{u} \cdot \nabla)\vec{u} + 2\vec{\Omega} \times \vec{u} = -\frac{1}{\rho}\nabla p + \mu \nabla^2 \vec{u} + \rho g \hat{z} \tag{1}$$

Where the terms are acceleration, advection, Coriolis force, pressure gradient, diffusion and gravity respectively. In both models we assume the system to be in a steady state and

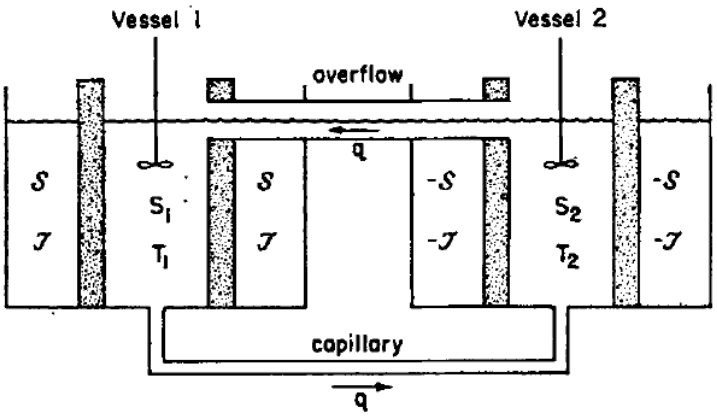

Figure 2: Simple schematic of the Stommel box model, from *Stommel (1961)*

working with a inviscid, hydrostatic and adiabatic fluid, which results in the geostrophic balance and the hydrostatic equation:

$$-f \cdot v = -\frac{1}{\rho}\frac{\partial p}{\partial x} \tag{2}$$

$$f \cdot u = -\frac{1}{\rho}\frac{\partial p}{\partial y} \tag{3}$$

$$0 = -\frac{\partial p}{\partial z} + \rho g \tag{4}$$

where f is the Coriolis parameter. The geostrophic balance, states that the Coriolis force is balanced by the gradient of the pressure field. Now this is where our models diverge.

Firstly we look at the box model proposed by Stommel (1961). Here he describes the ocean as two well mixed boxes connected in a upper layer overflow and a bottom capillary. These boxes are then seen as separate, with different temperatures, salinities and densities. The main assumption that Stommel makes is that the meridional velocity between these boxes is proportional to the meridional density gradient. If we assume no other surface forcing besides salinity and temperature, we can use scaling analysis to show this. Doing this Bryan (1987) ended up with a relation for the AMOC strength. We will not follow the exact steps of Bryan as we will continue in Cartesian coordinates, we will follow Vallis (2017) instead,

but the assumptions made and the result will be the same. We start by taking the vertical derivative of eq. (2) and inserting eq. (3):

$$\frac{\partial}{\partial z}(-f \cdot v) = \frac{\partial}{\partial z}(-\frac{1}{\rho}\frac{\partial p}{\partial x}) \tag{5}$$

$$f\frac{\partial v}{\partial z} = \frac{1}{\rho}\frac{\partial^2 p}{\partial z \partial x} \tag{6}$$

$$f\frac{\partial v}{\partial z} = \frac{1}{\rho_0}\frac{\partial \rho}{\partial x} \tag{7}$$

$$\tag{8}$$

We have arrived at the thermal wind relation. Now this is where a large inconsistent assumption is used. In Bryan (1987) he assumed that the zonal derivative could be exchanged with a meridional derivative. Doing this change and using scaling analysis we get:

$$f\frac{V}{D} = \frac{g}{\rho_0}\frac{\rho}{L} \tag{9}$$

Where D is the abyssal layer depth and L is the meridional length scale. We now define Stommel's two boxes, as we split the ocean into a tropical box and a polar box so we get:

$$f\frac{V}{D} = \frac{g}{\rho_0}\frac{\rho_2 - \rho_1}{L} \tag{10}$$

$$f\frac{V}{D} = \frac{g}{\rho_0}\frac{\Delta\rho}{L} \tag{11}$$

To do this we also assume the boxes to have different densities. To remove the unknown D from the relation, we use mass conservation for our two dimensional setup, as we have assumed zonal averaging, and Munk's (1966) advection-diffusion balance for temperature:

$$\frac{\partial v}{\partial y} + \frac{\partial w}{\partial z} = 0 \tag{12}$$

$$w\frac{\partial T}{\partial z} = k_T\frac{\partial^2 T}{\partial z^2} \tag{13}$$

Again we use scaling analysis, to get an equation for D:

$$\frac{V}{L} + \frac{w}{D} = 0 \tag{14}$$

$$w\frac{T}{D} = k_T\frac{T}{D^2} \tag{15}$$

$$\Rightarrow D = \frac{k_T L}{V} \tag{16}$$

Combining this with eq. (11) and defining the mass transport as the flux over the area we arrive at:

$$\Phi = VDL \tag{17}$$

$$\Phi = \frac{gD}{Lf\rho_0}\Delta\rho(\frac{fk_T\rho_0L^2}{g\Delta\rho})^{1/3}L \tag{18}$$

$$\Phi = (\frac{gL^4k_T^2}{f\rho_0})^{1/3}\Delta\rho^{1/3} \tag{19}$$

$$\Phi = \alpha \cdot \Delta\rho^{1/3} \tag{20}$$

The actual value of α is not important, but from Stommel's box model we find that there is a cubic relation between the AMOC and the density gradient. This means that from the Stommel box model closure of the geostrophic balance we find a relation of:

$$\Phi = a \cdot \Delta\rho^{1/3} + b \tag{21}$$

To find the precise relation described in Stommel (1961) one can do a first order Taylor expansion of the relation. This scaling and discretization was done in Bryan (1987), where he showed this one third relation, together with a two third relation of the vertical diffusivity. This relation is both somewhat empirical as it uses the Munk advection-diffusion balance (1966), and it also have a huge, non theory based, desperate, assumption in changing the derivative in the thermal wind balance.

Contrary to the box model where the AMOC is parameterized as described above, in the model described by Stommel and Arons in (1959) the strength and structure of the AMOC is defined and the horizontal flow is then calculated. If we go back and take the zonal derivative of eq. (2) and subtract the meridional derivative of eq. (3) we find:

$$\frac{\partial}{\partial x}(f \cdot u) - \frac{\partial}{\partial y}(-f \cdot v) = \frac{\partial}{\partial x}(-\frac{1}{\rho}\frac{\partial p}{\partial y}) - \frac{\partial}{\partial y}(-\frac{1}{\rho}\frac{\partial p}{\partial x}) \tag{22}$$

$$f_0(\frac{\partial u}{\partial x} + \frac{\partial v}{\partial y}) + \beta v = 0 \tag{23}$$

$$f_0\frac{\partial w}{\partial z} + \beta v = 0 \tag{24}$$

To get eq. (24) we have used mass conservation, and arrived at the Sverdrup relation. Now the key assumption in the Stommel Arons model is that the upwelling from the abyssal cold layer is uniformly distributed, meaning w will be uniform:

$$v = \frac{f_0 w_0}{\beta D} \tag{25}$$

From geostrophy we can then write the pressure as a zonal integral:

$$p = \int_{x_E}^{x} \frac{f^2 w_0}{\beta D} dx' \tag{26}$$

Since there is no flow at the eastern boundary, we can set $P = 0$ here and find:

$$p = -\frac{f^2}{\beta D} w_0 (x_E - x) \tag{27}$$

$$u = \frac{2}{D} w_0 (x_E - x) \tag{28}$$

We can now find the flow by firstly defining some source S_0 and using these velocities and mass conservation (this is for a basin going from equator to a northern pole and source):

$$S_0 + T_I(y) = T_W(y) + E(y) \tag{29}$$

$$T_I = \int_{x_W}^{x_E} vDdx = \frac{f}{\beta} w_0 (x_E - x_W) \tag{30}$$

$$E = \int_{x_W}^{x_E} \int_{y_N}^{y} w dx dy = w_0 (x_E - x_W)(y_N - y) \tag{31}$$

$$T_W = \frac{S_0}{y_N} (2y - \frac{f_0}{\beta}) \tag{32}$$

Where the first equation is mass conservation and T_I is the interior pole ward transport, E is the integrated loss due to upwelling and T_W is the equator ward transport at the western boundary. here we can see that in the Stommel Arons model we define the AMOC and solve.

Now the two models are clearly different as they are based on different key assumptions and they work in two different ways. Straub (1996) points out the inconsistency between the two models and show that the Stommel Arons model does not predict any relation between the meridional density gradient and the AMOC strength as found in Bryan (1987) from the Stommel box model. The Stommel Arons model is however dynamically consistent, and not

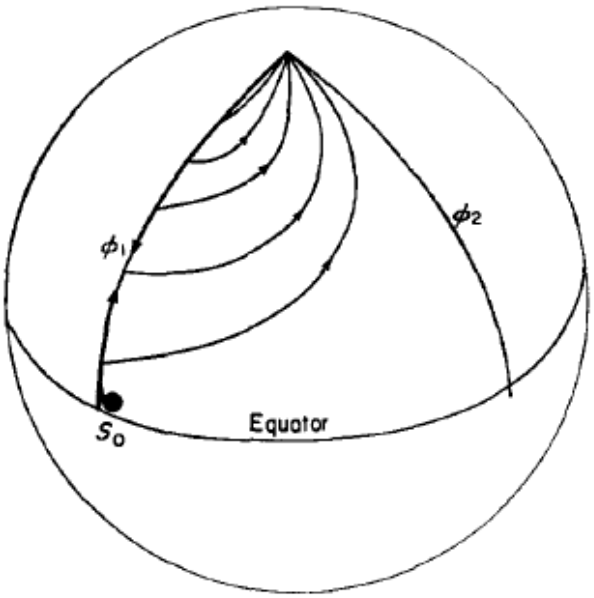

Figure 3: Simple schematic of the water structure in the Stommel Arons model, *Stommel Arons (1959)*

being able to merge this with the Stommel box model, hints that the assumptions made in Bryan (1987) are dynamically inconsistent. We will therefore in this thesis try to produce a relation between the AMOC strength and buoyancy forcing that is dynamically consistent, and therefore not use desperate assumptions such as the one made in Bryan (1987).

Lastly we would also like to include the wind stress forcing in the relation for the AMOC strength, and will therefore also analyse how a difference in windstress, specifically over the Antarctic ocean, affect the strength of the AMOC.

4

THESIS OUTLINE

The structure of this thesis will a bit alternative. After this *introduction* section, we will have a general *methodology* section, where the model used will be described, as well as the many different model setups done. After this we begin ***section I***, which will have its own *introduction*, where the Stommel box model closure found in Bryan (1987) will be tested, loosely following the method used in Greatbatch and Lu (G&L) (2003). Then We have a short *methodology* describing more specific runs for this experiment, followed by a *Results and analysis* where we check how to Stommel closure hold for different setups. After this we have a *discussion* where we compare our own results with that of G&L (2003) to see if we can support the claims made in the paper. Following this we have ***section II***, which will focus on a new closure instead of the Stommel box model. Again we will have a *introduction* describing the closure from Brüggemann and Eden (2011) (B&E). Same procedure as in ***section I***, as we again will have a *methodology*, *results and analysis* and a *discussion*, debating how well this new closure works and how it improves from the old. Then we have ***section III***, having the same chapter structure, where we will describe a new relation between the AMOC and atmospheric forcings, using the new closure. The penultimate section will be an overarching *discussion*, where we will look at all three experiments together, and discuss the problems and drawbacks of the old closure and what improvements follow with the new one. Lastly we have a *conclusion*.

Part II

METHODOLOGY

5

MODEL DOMAIN AND SETUP

To study the deep ocean stratification we will be running the ocean only model VEROS, described in Häfner (2018). VEROS is a primitive equation model written in pure Python based on the FORTRAN model pyOM2. VEROS simulates the Boussinesq equations of motion with full thermodynamics on a staggered Arakawa C-grid, meaning tracers and fluxes are calculated in different positions in all three dimensions. VEROS uses the finite difference approximation and a linear solver to solve the system. Our model will also have the turbulent kinetic energy model active, based on Gaspar (1990) for vertical mixing. Since VEROS is a pure ocean model, we will be running the model on both CPUs and GPUs.

Our model domain will be a idealistic version of the Atlantic ocean, With a long rectangular

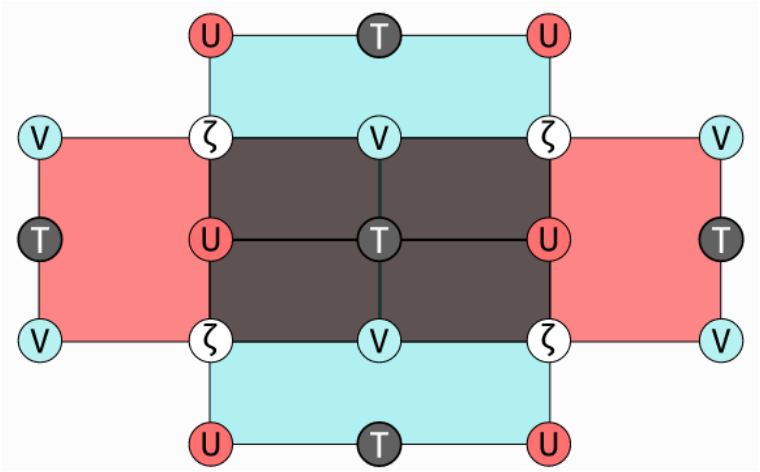

Figure 4: Schematic of tracers and momentum positions in a C-grid

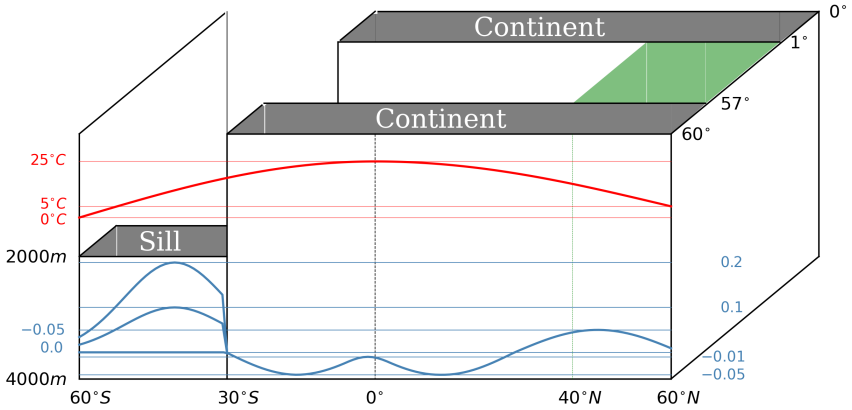

Figure 5: Schematic of the model basin and the forcings values and position

basin, with a channel in the south. We will base our model on that of Laurits S. Andreasen (2019). Our basin will have a width of 60 degrees and height of 120 degrees, going from 60 degrees south to 60 degrees north. The southern channel will be the bottom 30 degrees, where cyclic boundaries will be in effect. The depth of the model will be 4000 meters, however at the edges of the channel we will have a depth of 2000 meters to recreate the effects of the Drakes passage in the Southern ocean.

Since our model has full thermodynamics we will not be required to add any sources, we can instead add a general surface heat forcing. The surface will be relaxed with a wide sine wave, peaking at the equator with a value of 25 degrees Celsius and having a minimum of 0 degrees at the southern boundary and 5 degrees at the northern boundary. The heat forcing will have a relaxation timescale of 10 days. The model will have 40 layers in depth using a Vinkour grid refined towards the surface with initial interval of 10 meters. The model will initially be run in a coarse resolution of one degree by one degree. The model will have timesteps of one hour to make sure the Courant–Friedrichs–Lewy-criterion (CFL) is satisfied. We will also be running the model in a eddy resolving resolution of 1/6 degrees with a time step of 10 minutes. We will make use of VEROS inbuilt overturning output which is the meridional transport sampled 48 times a year.

To make sure the model reaches a steady state we will be running the coarse resolution for a 100 years to make sure the spin up is complete and the results are from a steady ocean. As the high resolution runs are costly, we will only be running these for 40 years, however they also reach a steady state.

The values changed in the runs will be the windstress, with a large focus on the windstress over the southern ocean, the horizontal friction and the salinity forcing. The wind, excluding over the southern ocean, is the same as described in Andreasen (2019), where most of the model setup is taken from, to mimic a simplified wind field over the Atlantic. The southern wind has a Gaussian peak around 40 degrees south and a e-folding of 15 degrees. The strength of the southern ocean winds varies with model runs, and some models will also have the wind outside of the southern ocean turned off. The Horizontal friction changes will be discussed in the next section. The salinity forcing will be varying, only be on the upper 20 degrees and will be uniform, with a timescale of 10 days. This forcing is to force a AMOC cell to appear even for low horizontal frictions. In the real world the salinity decrease towards the north, however if we do this, the AMOC cell will turn off, and we therefore decide to increase it instead.

Part III

SECTION I

6

INTRODUCTION AND THEORY

In this section we will analyse the inconsistency between the Stommel Arons model and the Stommel box model as noted in Straub (1996). We will base our work on that of G0&L (2003), who used a simple two layered model to analyse this inconsistency. Here they simulate a simple rectangular basin with a southern ocean channel to signify the Atlantic to see if there is any relation between the meridional density gradient and the AMOC strength. To do this they simulate for different values of a parameter R and then compare the meridional transport with the layer displacement height. The closer these are linked the more it supports Stommel's box model and in turn the relation found in Bryan (1987). The parameter R in question is the ratio between the propagation time scale to the dissipation time scale in the model and will be a key parameter in this thesis. In other words the ratio between the wave (mostly Kelvin waves) time scale and the time scale associated with the horizontal friction. This will tell us what is dominant in our ocean. For $R << 1$ we are in a weak dampening scheme and the Kelvin (and Rossby) waves will dominate and distribute the information around the basin and to the interior. When we have $R >> 1$ we are in the strong dampening scheme and the horizontal friction will kill of most of the waves and dominate. This can also loosely translate to numerical model resolution, as we need the weak dampening to resolve eddies, however for low resolution models there can be problems. R is

more precisely calculated as the ratio between the Kelvin wave timescale and the horizontal friction timescale:

$$R = \frac{T_k}{T_D} \tag{33}$$

$$T_k = \frac{L}{c} \tag{34}$$

$$T_D = \frac{L_D^2}{A_h} \tag{35}$$

$$R = \frac{L \cdot A_h}{c \cdot L_D^2} \tag{36}$$

Where L is the kelvin wave length scale, L_D is the dissipation length scale, c is the kelvin wave speed and A_h is the lateral viscosity or horizontal friction. In G&L (2003) they vary the parameter R for different setups with different water source strengths and different southern ocean windstress. R is changed by using different linear horizontal frictions. They draw two main conclusions. Firstly they find that with no southern ocean windstress and no channel, the model is in the Stommel Arons regime for $R << 1$ and in the Stommel box regime for $R >> 1$ with the latter breaking down around $R = 1$. This means they find that for high dampening there is a relationship between the meridional density gradient and the AMOC strength, while this is not the case in the weak dampening regime. Secondly they find that with a channel and increasing the southern ocean wind stress, the model tends to move towards to Stommel box regime even for lower R values. This means that they find southern ocean wind stress to strengthen the relation between the meridional density gradient and the AMOC strength.

We will in this section use this R parameter to see if there is a dependency on how strong the relation between the AMOC and the density gradient found in Bryan is, and test how the southern ocean wind stress affects this. We will use a primitive equation model with thermodynamics instead of just a two layered model. This also means we will not have need for any water sources as in G&L (2003).

7

METHODOLOGY

The model domain has already been described in the previous section, however we will here go through the specific model values for the three main variables that will change. The parameters: Windstress, Salinity forcing and horizontal friction (the R parameter) is what will be changing. As in G&L (2003) we would like to test how R affects the relation from Bryan (1987). We will therefore run models of both high R values and low R values. Now to estimate R from the Horizontal friction we use eq. 36. We estimate the kelvin wave length scale, L, to be 25000 km which is a rough estimate of the distance the Kelvin wave has to travel. The dissipation length scale we estimate to be around the grid spacing of approximately 111 km. The wave speed, c, is approximated to be $c = \sqrt{g'H}$, where g' is the reduced gravity of around 0.01 and H is the upper layer thickness which is around 100 m. This gives us an estimated wave speed of 1. All this gives us a relation between R and A_h of:

$$R = \frac{L \cdot A_h}{L_D^2 \cdot c} \approx A_h \cdot 2 \cdot 10^{-3} \tag{37}$$

Now we want to vary R to be in both the weak dampening regime and the strong dampening regime. The chosen values are shown in table 1. Secondly we want to explore G&L's (2003) second point of southern ocean windstress. We will therefore run for the parameters for the magnitude of the Gaussian peak in the southern ocean shown in table 2. Now, to test the relation between the AMOC and the density gradient we will need multiple model runs

R [$unitless$]	A_h [$m^2 s^{-1}$]
0.01	$5 \cdot 10^0$
0.1	$5 \cdot 10^1$
1	$5 \cdot 10^2$
10	$5 \cdot 10^3$
100	$5 \cdot 10^4$

Table 1: Horizontal friction values

Name	τ_0 [Nm^{-2}]
Wind 1	0
Wind 2	0.1
Wind 3	0.2

Table 2: Southern ocean windstress values

with the same wind and R value. We therefore vary the salinity forcing in the upper 20 degrees, to simulate different strengths of the AMOC as shown in table 3. In the real world the salinity forcing would be lower in the north, however we need to force a AMOC cell, and will therefore be increasing it. The theory should still hold. 35 is the standard forcing. All salinity forcings will be run for all R values, which will be run for all windstresses. The names will then be denoted like the following example: w1r01s_3 is for the windstress of 0.0, an R value of 0.1 and a salinity forcing of 38. If no s_# is added then it is implicit s_0.

In G&L (2003) they compare the interface height displacement with the AMOC strength at all latitudes. It is not possible to make such a comparison in any meaningful way for our setup. We will therefore instead find a single AMOC strength value and single density gradient value to compare per run. How these are found will be discussed later.

We expect some grid-scale noise for the lower viscosity runs, and we will try to average

Name	S_0 $[PSU]$
salt 0	35
salt 1	36
salt 2	37
salt 3	38
salt 4	39
salt 5	40

Table 3: salinity forcing values

this away using a two point box car filter. This will however have a possible large effect as grid-scale noise can induce grid-scale friction, which will then alter the true horizontal friction present in the system as described in Jochum (2008). We will therefore also be running a setup of High resolution eddy resolving models at 1/6 th degree resolution, to test if this induced grid scale noise affects the results significantly. These models will have wind 1 and a R value of approximately 0.2, meaning it will be in the low dampening scheme.

8

RESULTS AND ANALYSIS

One of the big assumptions we make is that the models have reached a steady state, and therefore no longer have any large temporal fluctuations. As can be seen from fig. 6 the models reach a steady state after around 10 years, so the long spin up of 100 years (and the high resolution spin up of 40 years) is more than enough the ensure this assumption is valid. Nonetheless we do still have some temporal oscillation, which we will average out, by taking the average of the last five model years, as shown by the dotted lines. This will be done after the box car filter discussed earlier.

To test the Stommel box model closure, specifically the density gradient part of it, we need to firstly chose a way to determine the strength of the AMOC. We chose 20 degrees North as the latitude where we will be measuring the AMOC strength, as we will see a cell of varying intensity for most of the model runs and we will see a change in strength. We also assume this value will be representable of the strength of the entire AMOC and do not expect any positional bias. Depth wise, we decide on a little flexibility, and will find the maximum value between 250 meters and 2100 meters depth, as this is the range where the AMOC cell will be for the model runs at the chosen latitude. A few model runs are shown in fig. 7. The overturning is in Sverdrup.

Now the second thing we need to find is the density difference of the two boxes. Here we will follow Guido et al. (2022) on how to define the boxes. Firstly we will only be using

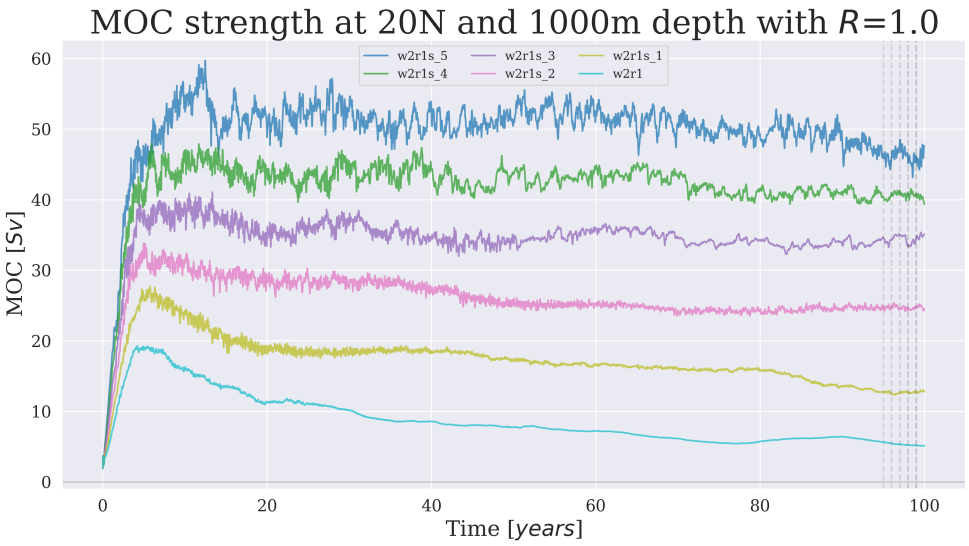

Figure 6: Time series of a arbitrary set of model runs

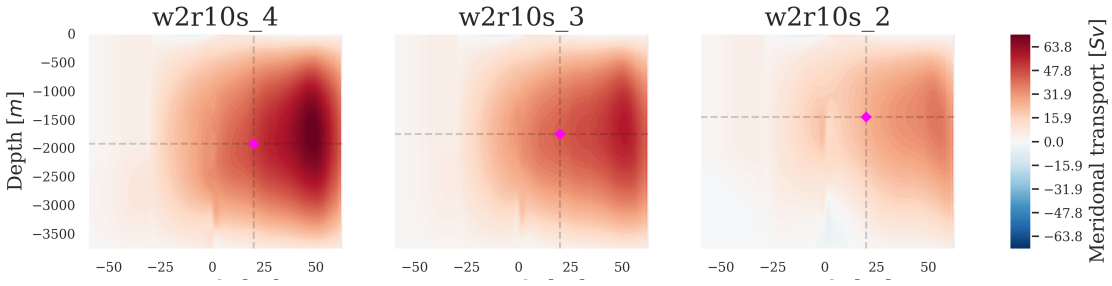

Figure 7: Meridional overturning circulation with measured point of a arbitrary set of model runs

the surface layer, as we want the density gradient to be a function of atmospheric forcings, and this way we can describe it as a atmospheric boundary condition. this way we also separate it as much from the AMOC as possible. Following Guido et al. (2022) we split the Atlantic into a southern box and a northern box, to mimic the Stommel setup. The northern box will go from 40 degrees north and up, to make sure we get no affect from the equator. The southern box will be a bit smaller, as we also want to be away from the equator, but we also need to be above the channel, and not have any of the sharp density gradient from the edge of the channel do to Ekman suction. We therefore define it from 20 degrees south to 15 degrees south. We also follow Guido et al. (2022) by using buoyancy forcing instead of density, by using:

$$\Delta b = -\frac{g}{\rho_0}\Delta\rho \tag{38}$$

Where g is the gravitational acceleration, ρ_0 is the standard seawater density which we define as 1024 $\frac{kg}{m^3}$ and $\Delta\rho$ is the difference between the density of the south Atlantic and north Atlantic boxes.

We are then able to test the relation of $AMOC = a \cdot \Delta b^{1/3} + b$. We start by looking at the models with no southern ocean winds in fig. 8. Here we see that for very low R values, the fit is not perfect, but it does still capture the trend. As R increase the fit becomes a better representation of the data, and from $R = 1$ and up, the fit captures the trend of the data. In fig. 9 and fig. 10 we see the same plot for the windstress of 0.1 and 0.2. We here see the same thing, however we see that even for the very low R value, the fit is still a fine representation of the data, and that for the higher R value, the data is very well captured.

In fig. 11 we compare runs for the highest R value of different windstresses. What we see is that the southern ocean wind stress has a additive effect on the relation between the AMOC strength and the buoyancy gradient. This means we can treat the buoyancy forcings and the windstress forcing in a superposition.

Lastly we also want to use the eddy resolving runs. As stated earlier there is some numerical

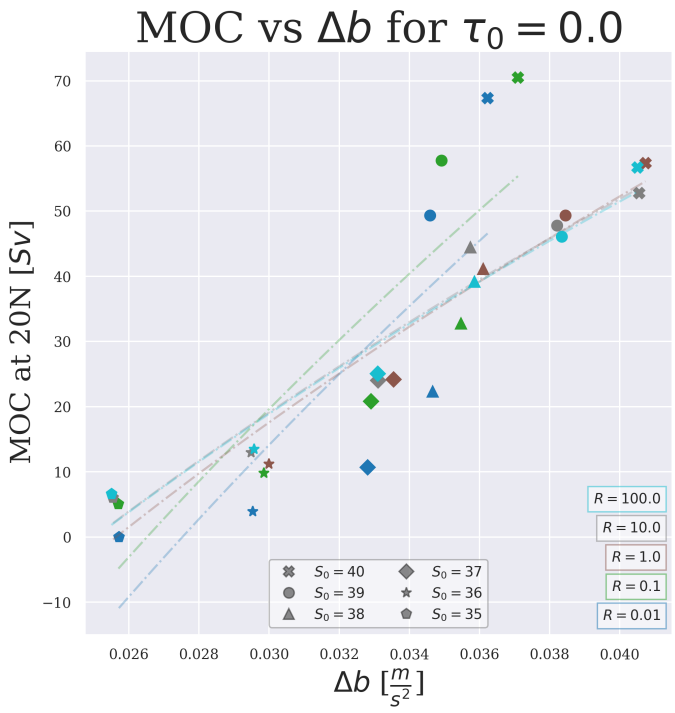

Figure 8: Meridional overturning circulation plotted against the buoyancy forcing for the model runs of w1

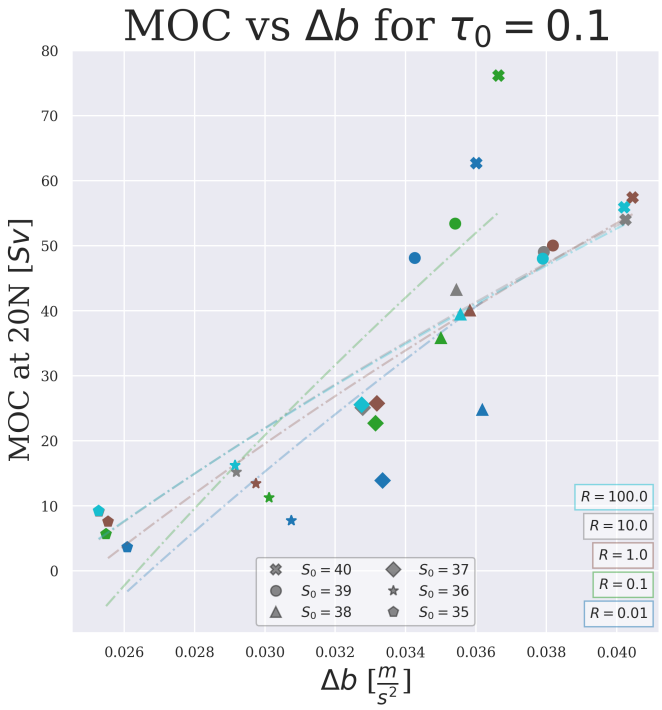

Figure 9: Meridional overturning circulation plotted against the buoyancy forcing for the model runs of w2

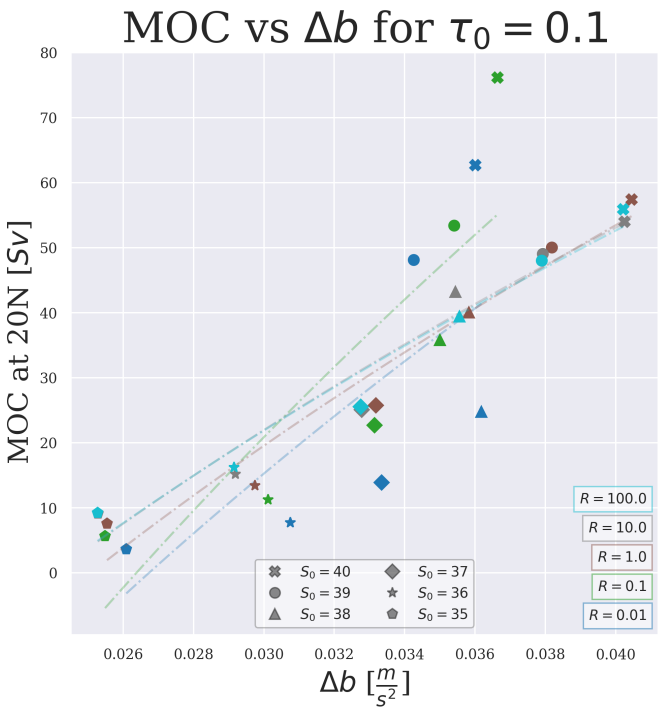

Figure 10: Meridional overturning circulation plotted against the buoyancy forcing for the model runs of w3

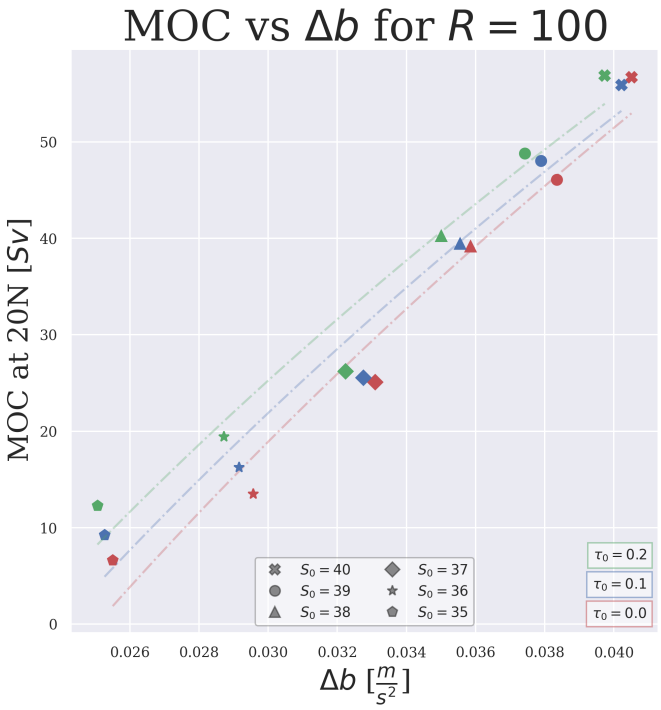

Figure 11: Meridional overturning circulation plotted against the buoyancy forcing for the model runs of $r = 100$

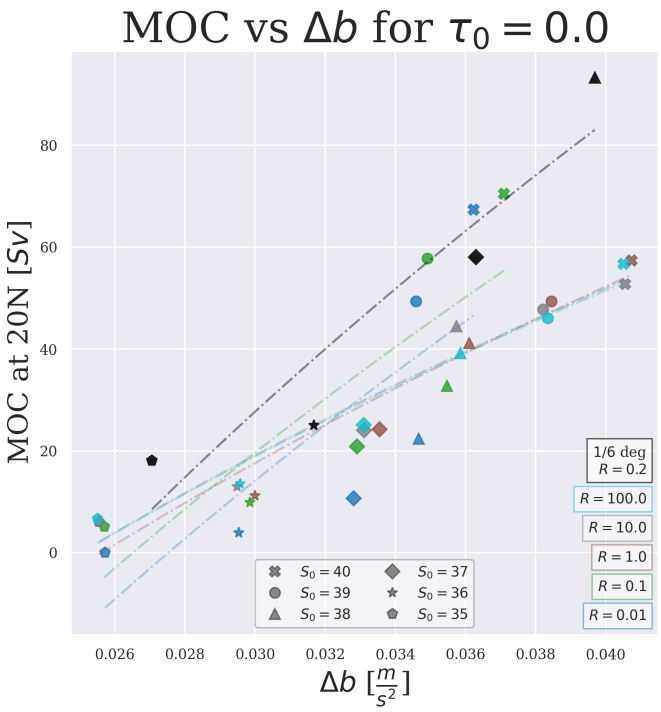

Figure 12: Meridional overturning circulation plotted against the buoyancy forcing for the model runs of w1, including the eddy resolving models

noise in the coarse resolution models with low horizontal friction. This numerical noise can induce a numerical friction, which will then change the actually horizontal friction in the system. We therefore use the eddy resolving model, to see if it matches well with the results from the coarse resolution models. If this is the case we can assume that the numerical friction in negligible. The high resolution runs are done with no southern ocean windstress, so a comparison with the coarse resolution runs with the same winds are shown in fig. 12. we see that the eddy resolving model relation, does not have any large differences from the coarse resolution. The fit captures the data well, and the parameters of the fit are within range of the coarse resolution parameters. We do however see that the AMOC strength is generally higher. from this we can assume that the coarse resolution results are good and the numerical friction is negligible as the eddy resolving model does not show any largely different results.

9

DISCUSSION

This section is about analysing how well the relation between the AMOC and the buoyancy gradient proposed in Bryan (1987) based on Stommels box model, holds for a primitive equation model using the Boussinesq equations and thermodynamics. We used the study conducted in G&L (2003) as a basis, and the parameter, R, they defined. The first major claim made in G&L (2003) was that the Stommel box model does not hold for low horizontal friction, i.e. $R << 1$, but only when $R >> 1$. As we discussed earlier and can be seen in fig. 12 this is not the case in our model. We do see that the relation based on the Stommel box model is not great for $R = 0.01$, it is however still a fair fit for the general trend of the data. now for $R = 0.1$ and $R = 1$ we see that the relation does describe the data well, and it is therefore a good fit. This is in direct contrast with the claim made in G&L (2003), as we believe the Stommel box model relation describes the system well, even for low R. Now G&L (2003) does only use a simple two layered model, so this could be why we see this difference. One could say that our claims are based on coarse resolution runs and the numerical noise could therefore be the reason that we see the Stommel relation hold even for low R values, as they might not actually be low due to numerical friction. However we argue that this is not the case, as we have also tested the relation on a eddy resolving model with low R value, and found it to be consistent with our previous coarse resolution results. We can therefore not support this claim made in G&L (2003).

The second claim made in G&L (2003) was that southern ocean wind stress has a strengthening effect on the relation between the AMOC and the buoyancy gradient. We do not find this to be the case for higher R value, but for low R value, the fit does describe the trend of the data for higher wind stress somewhat better than for lower. We can however not support this claim on this little evidence. However we do find southern ocean wind stress to have an impact. We find that the windstress is in a superposition with the buoyancy forcing, and therefore seems to have a linear impact on the AMOC.

Part IV

SECTION II

10

INTRODUCTION AND THEORY

One of the big faults of the Bryan (1987) closure is the assumption that you can shift out the zonal gradient with a meridional one, which is not the case for most of the ocean. We will therefore in this section look into a alternative closure proposed in B&E (2011). Here instead of using the Stommel box model and split the ocean into a southern and northern box, they instead propose a zonal split. The ocean is split into a western boundary box and an interior box, which are then zonally averaged separately. This would mean that instead of having a expensive three dimensional prognostic model, you could get away with having two coupled two dimensional models, which we will call 2.5 dimensional. The B&E (2011) closure is also dynamically consistent compared to the Stommel one. The B&E (2011) closure builds on a zonal split between the western boundary and the interior of the ocean, and results in the following main assumption:

$$B\bar{v} = B_b\bar{v}_b + B_i\bar{v}_i \tag{39}$$

Here B is the zonal length of the basin and the subscripts means boundary and interior respectively. This closure builds a zonally averaged model, And we therefore start by taking

the zonal average of the momentum equations and the continuity equation over each box separately, to get:

$$\frac{\partial \bar{u}_\alpha}{\partial t} - f\bar{v}_\alpha = -\frac{1}{\rho_0}\frac{\Delta p_\alpha}{B_\alpha} + \bar{F}^u_\alpha \tag{40}$$

$$\frac{\partial \bar{v}_\alpha}{\partial t} + f\bar{u}_\alpha = -\frac{1}{\rho_0}\frac{\partial \bar{p}_\alpha}{\partial y} + \bar{F}^v_\alpha \tag{41}$$

$$\frac{\partial \bar{b}_\alpha}{\partial t} + \frac{\partial \bar{b}_\alpha}{\partial y}\bar{v}_\alpha + \frac{\partial \bar{w}_\alpha}{\partial z}\bar{b}_\alpha = \frac{\partial K_\alpha}{\partial z}\frac{\partial \bar{b}_\alpha}{\partial z} - \epsilon_\alpha u_\delta \frac{\bar{b}_\alpha}{B_\alpha} \tag{42}$$

$$\frac{\partial \bar{v}_\alpha}{\partial y} + \frac{\partial \bar{w}_\alpha}{\partial z} = -\epsilon_\alpha \frac{u_\delta}{B_\alpha} \tag{43}$$

Here the subscript α can be b or i and the $\bar{F}$ terms contain all the friction terms, and will be described later. Here B&E (2011) define some parameterizations for the pressure gradients to close the set of equations:

$$u_\delta = \gamma_1 \bar{u}_b \tag{44}$$

$$\Delta p_i = \rho_0(\Delta p_i(y=0) + \gamma_1 \int_0^y f\bar{u}_b dy') \tag{45}$$

$$\Delta p_b = \gamma_2(\bar{p}_i - \bar{p}_b) \tag{46}$$

Here two tuning parameters are defined. The first parameterization is made as they demand that the thickness balance for the interior regime yields the averaged form of the Sverdrup balance. This demand is made by the first parameterization (for more detail see B&E (2011)). The integration constant $\Delta p_i(y=0)$ can be found be using the steady version of the zonal momentum balance at the equator. The second parameterization is a simple ansatz. Our goal is to describe a model for the AMOC and would therefore like to use their model and parameterization to find a equation for the AMOC based on their 2.5 dimensional model. The AMOC strength we define as the meridional flux:

$$\Phi = h(B_b\bar{v}_b + B_i\bar{v}_i) \tag{47}$$

Now as we are looking at the steady state, we set the acceleration term to zero and isolate the meridional velocity in the steady momentum equations and insert them:

$$\Phi = \frac{h}{f}(\frac{1}{\rho_0}(\Delta p_b + \Delta p_i) - (B_b \bar{F}^u_b + B_i \bar{F}^u_i)) \tag{48}$$

We chose to neglect the $\bar{F}^u_\alpha$ terms, as the diffusive and viscous terms are small. The windstress will also be part of the $\bar{F}$ terms, but for now we assume no wind stress. We now have 2.5 dimensional zonally averaged set of equations to find the AMOC as a function of the pressure field. This set of equations are still prognostic and need to evolve in time, but they are only 2.5 dimensional and therefore much faster than a expensive three dimensional model.

11

METHODOLOGY

The goal of this section is to see if the closure from B&E (2011) can be used as a dynamically consistent prognostic zonal averaged 2.5 dimensional model. For this we will be analysing the north Atlantic, and here we can use the model runs already described in earlier sections. We will make use of the high resolution runs and compare the AMOC found using the derived equations and compare this to the output directly from VEROS. We will however do a new run to simplify things even more. We will do a coarse resolution run with no wind forcing at all, with a R value of 100 and a salinity forcing of 38.

From the model runs we will use the density output directly from VEROS to compute the pressure field. We can also safely assume no wind forcing term for the coarse resolution run. We will also make use of the stream function from VEROS to calculate the western boundary width, as this is needed to split the ocean into the two boxes. Here we will define the boundary width as the first minimum of the stream function at 20 degrees north as this should encapsulate both the northward flow and the return flow. The value found for the coarse resolution run, will then also be used for the high resolution run, as a quick estimate of the boundary width.

12

RESULTS AND ANALYSIS

We start by looking at the coarse resolution run with no wind stress. In fig. 13 we see the three parameterizations from the B&E (2011) closure. When comparing these to the results from the paper we see a good resemblance for most of it. The Δp_b is as seen calculated from the pressure field, while the others are calculated from the zonal velocity field. We see a strong positive cell in Δp_b with a strong negative cell below it. In Δp_i the most notable features are the positive cell in the lower right corner, and the negative cells in the outer upper ocean. When these parameterizations are then used to calculate the AMOC, we see a good resemblance with the AMOC directly from VEROS shown in fig. 14. We see a strong positive cell going from a couple meters depth down to the bottom, in both the AMOC calculated from the closure and the AMOC from VEROS. Both cells do also reach

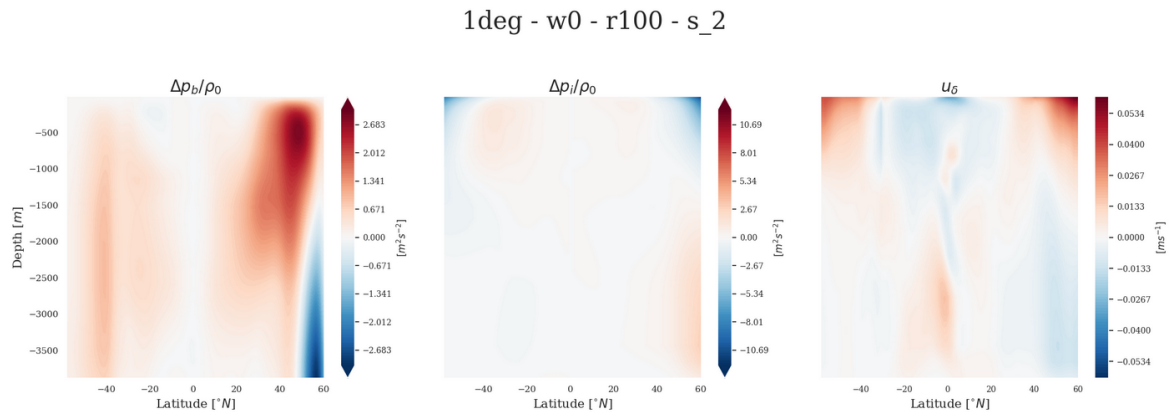

Figure 13: The three parameterizations from the B&E (2011) closure for the 1 deg model

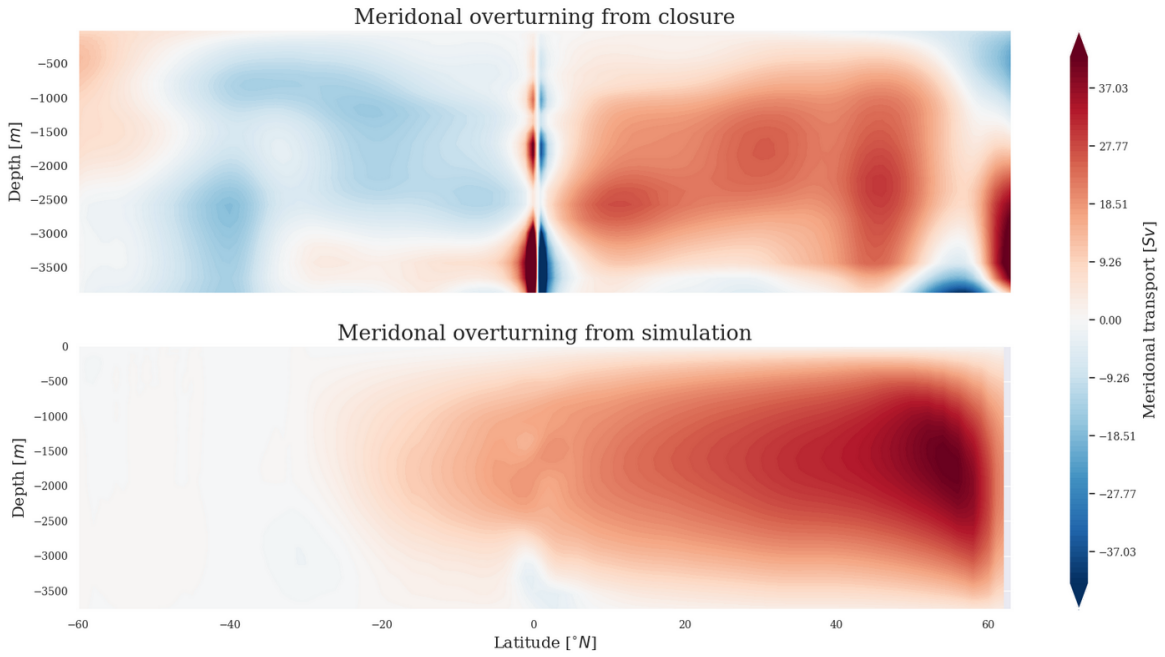

Figure 14: The overturning calculated from the closure and the overturning from VEROS for the 1 deg model

the northern boundary, where they both strengthen towards to bottom of the ocean. The big difference between the two is at around 55 degrees north, where the calculated cell weakens drastically, however it is still positive. This is due to the fact that the negative bottom cell in Δp_b is wider than the positive bottom cell in Δp_i. However the cell is still positive in this section, so it can be seen as one large cell in stead of two, meaning a very good resemblance between the AMOC from the closure and the AMOC from VEROS for coarse resolution.

One thing we need to chose is the tuning parameters. We use 1 and 1.5 for γ_1 and γ_2 respectively. This matches good with the values found in the B&E (2011) paper of 1.2 and 1.7. These tuning parameters can roughly be seen as tuning the strength of the parameterizations Δp_i and Δp_b respectively. Meaning when you increase γ_1 you also increase Δp_i and in turn the AMOC will look more like this parameterization. Now for the coarse resolution we were able to get good results using tuning parameterization very similar to the ones found in B&E (2011). This was however not the case for the high resolution runs. As will be describe below, the Δp_i was a good match and we therefore kept the tuning parameter of 1, however

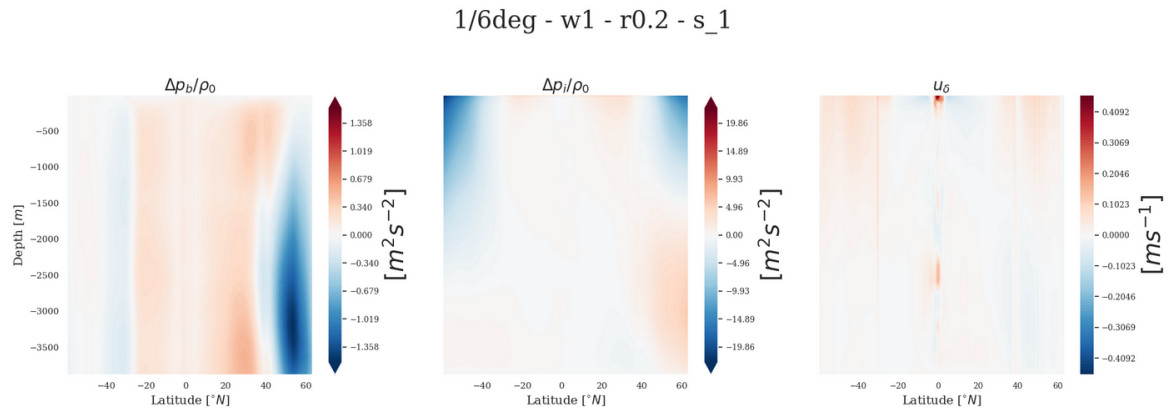

Figure 15: The three parameterizations from the B&E (2011) closure for the 1/6 deg model

because the Δp_b parameterization change so much, we needed to minimize its impact on the AMOC while still keeping it relevant, and landed on a value of 0.2 for γ_2.

When looking at the eddy resolving models, the Δp_i and u_δ parameterizations match well with B&E (2011) and the results found from the coarse resolution run as seen in fig 15. However there is a large discrepancy in the Δp_b parameterization. In all high resolution runs the lower negative cell is dominating most of the north Atlantic. This means that the gradient between the interior and boundary pressure fields are not well balanced. This large negative cell offsets the AMOC. The cell in the coarse resolution made sure the AMOC was not bottom intensified, however in these high resolution runs, it more or less destroys the AMOC, as shown in fig. 16. As we have turned the tuning parameter down for the Δp_b to try and mitigate the damage and to make sure it does not completely remove the positive lower cell seen in the Δp_i parameterization, we only see a smaller, bottom intensified northern AMOC cell for all of the high resolution cells.

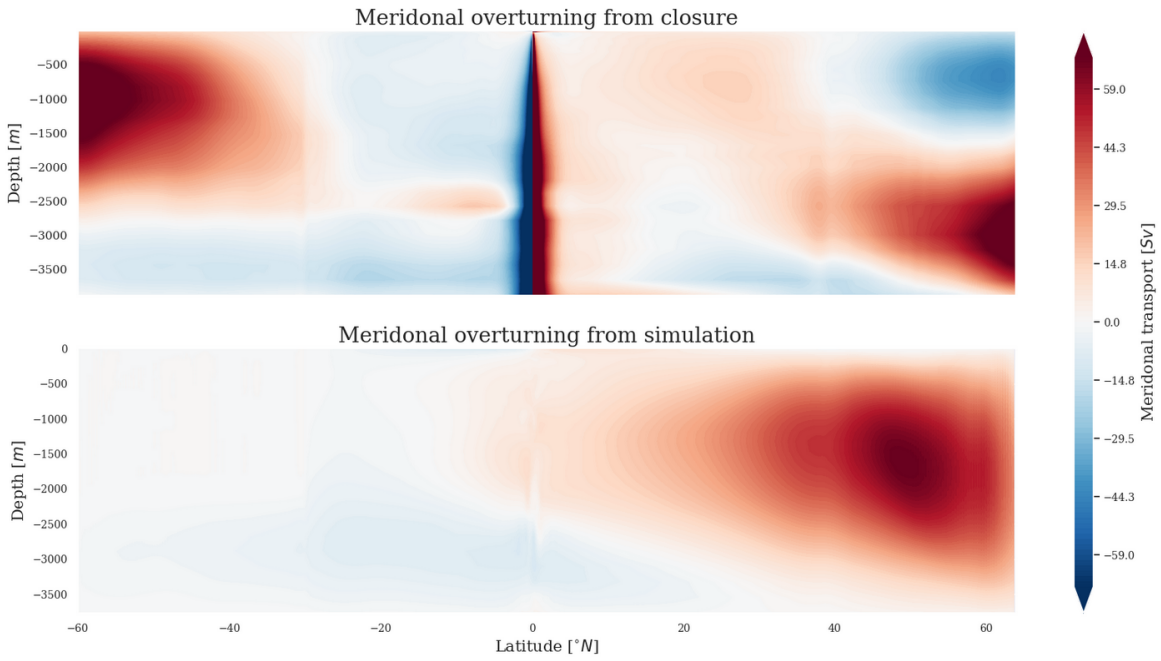

Figure 16: The overturning calculated from the closure and the overturning from VEROS for the 1/6 deg model

13

DISCUSSION

The B&E (2011) closure uses two coupled zonally averaged models and are therefore much faster to evolve in time than a expensive three dimensional one. We have shown that in coarse resolution this 2.5 dimensional model is a good substitute, and you are able to recreate the AMOC from the Closure. We do see some differences, however the strength and form of the AMOC cell are mostly the same. We also see that in coarse resolution you can safely ignore the nonlinearities. You do need to define tuning parameters for this closure however. We see that for a coarse resolution models tuning parameters around unity (1 and 1.5) does recreate the AMOC nicely.

Now for the high resolution models we do see large discrepancies between the AMOC found from the closure and the AMOC directly from VEROS. As stated earlier this is largely due to the parameterization Δp_b, which have a large negative cell for most of the north Atlantic. This indicates that the pressure (and in turn density) gradient between the two boxes are far to large, and uniform throughout the water column. From this we can not recommend using this simplified version of the B&E (2011) closure for eddy resolving models. However if one were to include the non linear terms for the calculation, we expect that the result would improve greatly, as we see the closure does reproduce the AMOC for the coarse resolution model.

We would therefore recommend the B&E (2011) closure as a faster prognostic model as it

is 2.5 dimensional for coarse resolution, where you can safely ignore the nonlinearities for modeling the AMOC. For eddy resolving models we expect the closure to work well if the nonlinearities are included, but we can not show this. We however see that the closure does not work for high resolution models when these terms are ignored.

Part V

SECTION III

14

INTRODUCTION AND THEORY

The current relation between the strength of the AMOC and the buoyancy forcings, has it fair share of problems as shown earlier. We will in this section propose a new closure to get a relation, broadly following the steps of Bryan 87, but without the assumption of switching the derivative. We have also tested the B&E (2011) closure, and we see that, at least for coarse resolution, it recreates the AMOC well from the density field. We therefore started going from this closure. However after multiple attempts at closing a simplified version of the B&E (2011) closure we found that this was not possible (See appendix *closures* for further detail). Nevertheless This new closure will take its starting point in the zonal splitting of the ocean as proposed in B&E (2011). We again start from the geostrophic balance, specifically for the boundary box:

$$f v_b = \frac{1}{\rho_0}\frac{\partial p}{\partial x} \tag{49}$$

$$f\frac{\partial v_b}{\partial z} = -\frac{g}{\rho_0}\frac{\partial \rho}{\partial x} \tag{50}$$

We have rewritten to the thermal wind relation using the hydrostatic relation. We then do scaling of the equation:

$$f\frac{V_b}{D} = \frac{g}{\rho_0}\frac{\rho_b - \rho_i}{B} = \frac{g\Delta^x\rho}{\rho_0 B} \tag{51}$$

Where D is the layer height, B is the width of the boundary layer, V_b is the meridional flow in the boundary layer, ρ_b is the density in the boundary and ρ_i is the density in the interior. Here

we make the assumption that in the abyssal layer all water going south in the north Atlantic is in the boundary layer, and as in the Stommel Arons model all the water going north is in the interior. Going on this assumption we know that all southward going flow is made and submerged in the polar region and we can therefore say that $\rho_b = \rho_{pole}$. This means we can find the density in the boundary directly from atmospheric boundary conditions. Now using the Stommel Arons model we know that the flow going north throughout the interior is the water originally submerged in the polar region. We now assume that the most important and dominating process affecting the density is diffusion. We therefore propose the simple parameterization:

$$\rho_i = \rho_{pole} - \frac{\Delta^z \rho}{D} \cdot \kappa_T \cdot \Delta t \tag{52}$$

Where κ_T is the vertical diffusivity, Δt is the time scale of the density modification and $\Delta^z \rho$ is the vertical density difference. Now we know the abyssal density is the water submerged at the polar region. The upper surface water is equal to the upwelling in the tropics. We can therefore make the following relation:

$$\Delta^z \rho = \rho_{surface} - \rho_{abyssal} = \rho_{tropic} - \rho_{pole} = \Delta^y \rho \tag{53}$$

As we see, this way we can get the meridional density difference sought after in Bryan (1987), without making the desperate change in density gradient. Inserting this:

$$V_b \cdot B = \frac{gD}{f\rho_0}(\rho_{pole} - (\rho_{pole} - \frac{\Delta^y \rho}{D} \cdot \kappa_T \cdot \Delta t)) \tag{54}$$

$$V_b \cdot B = \frac{g\kappa_T}{f\rho_0}\Delta^y \rho \cdot \Delta t V_b \cdot B = \frac{g\kappa_T L}{f\rho_0 V_i}\Delta^y \rho \tag{55}$$

Here we define the time scale of the density modification simply as the meridional length over the interior flow velocity. To find a relation for the interior flow velocity we use Munk's

advection-diffusion balance for temperature and the Sverdrup balance (we do not use mass conservation as in Bryan (1987), see appendix *closures*):

$$w\frac{\partial T}{\partial z} = \kappa_T \frac{\partial^2 T}{\partial z^2} \rightarrow w = \frac{\kappa_T}{D} \tag{56}$$

$$\beta v_i = f\frac{\partial w}{\partial z} \rightarrow \beta V_i = f\frac{w}{d} \tag{57}$$

$$V_i = \frac{f\kappa_T}{\beta D^2} \tag{58}$$

This is very close to the relation found in Bryan (1987), when you see f/β as a length scale. With this relation, we can find a relation for the layer depth, by utilizing the assumption of all the flow going south in the boundary is going north in the interior:

$$V_i \cdot L = V_b \cdot B \tag{59}$$

$$\frac{f\kappa_T L}{\beta D^2} = \frac{g\kappa_T L}{f\rho_0 V_i}\Delta^y \rho \tag{60}$$

$$\frac{f}{\beta D^2} = \frac{g\Delta^y \rho}{f\rho_0}\frac{\beta D^2}{f\kappa_T} \tag{61}$$

$$D^4 = \frac{f^3}{\beta^2}\frac{\rho_0 \kappa_T}{g\Delta^y \rho} \tag{62}$$

With this we can find a relation for the overturning strength:

$$\Phi = V_b \cdot B \cdot (H - D) = V_i \cdot L \cdot (H - D) = V_i \cdot L \cdot H \cdot (1 - \frac{D}{H}) \tag{63}$$

$$\Phi = \frac{f\kappa_T}{\beta D^2} \cdot L \cdot H \cdot (1 - \frac{D}{H}) \tag{64}$$

$$\Phi = \frac{f}{\beta}\kappa_T \cdot L \cdot H \cdot (\frac{\beta^2}{f^3}\frac{g\Delta^y \rho}{\rho_0 \kappa_T})^{1/2} \cdot (1 - \frac{D}{H}) \tag{65}$$

$$\Phi = (\frac{gL^2H^2}{f\rho_0})^{1/2} \cdot \kappa_T^{1/2} \cdot \Delta^y \rho^{1/2} \tag{66}$$

Where H is the total water column height and L is the meridional length. We end up with a relation close to that of Bryan (1987), however we end up with a squared relation instead of the cubic relation found in the paper. We also assume that $D << H$.

We now have a dynamically consistent, semi empirical (due to the Munk relation) relation between the AMOC strength and the buoyancy forcing. This would be a big improvement on the relation found in Bryan (1987), as we here do not use the very loose and dynamically

inconsistent assumption of changing the zonal density gradient to meridional. In this section we want to check how well this new fit holds up, similarly to what was done in section one. We want to use the buoyancy gradient as done in section one, however we also want to check the relation for the vertical diffusivity as done in Bryan (1987).

15

METHODOLOGY

We will be using the already described coarse resolution runs and the eddy resolving runs, to test the relation between the AMOC and the buoyancy forcing as done in section three. However we will also be using the vertical diffusivity and see how the relation between this and the AMOC strength holds up. As shown in Bryan (1987), a change in vertical diffusivity will lead to a large difference in AMOC, and we will therefore, hopefully, be able to take a closer look at the difference between this new fit and the old one.

We will be running an additional four models based on the coarse resolution run with no wind, a strong horizontal friction with an R value of 100 and a salinity forcing of 38. This is chosen due to the numerical stability and the strong overturning. The vertical diffusivity has so far been set to $2 \cdot 10^{-5} m^2/s$. We will be making large changes, factors of ten, as we want to see a difference between a cubic (2/3 will be called cubic for convenience) and squared function. We therefore will use the values sown in table. 4. $k1$ is then the model already described earlier.

Name	κ_T $[m^2 s^{-1}]$
k001	$2 \cdot 10^{-7}$
k01	$2 \cdot 10^{-6}$
k1	$2 \cdot 10^{-5}$
k10	$2 \cdot 10^{-4}$
k100	$2 \cdot 10^{-3}$

Table 4: Vertical diffusivity values

16

RESULTS AND ANALYSIS

The data we will fit the new closure to is the same as used in section one, and how it is defined and collected is described in that section. We test the relation of $AMOC = a \cdot \Delta b^{1/2} + b$. As can be seen in fig. 17 the new fit is almost identical to the previous relation. Again we see that for the lowest R values, the fit is not great, but it does capture the general trend of the data. We also see that for the other R values, the fit is a good match for the data. for a more descriptive analysis of the fit against the data, see section one as, in this interval at least, the new fit is identical to the old fit.

Nevertheless since the two fits are different polynomials, the parameters are different as seen in fig. 18. We see that a general shift upwards is the case for both parameters going from the cubic to the squared function. This can however be explain as the constants in the relation are different. Again we also see the windstress having a additive effect. In fig. 19 we see that the eddy resolving model is no different and the fit captures this well to.

Now a cubic and a squared function are quite similar when the interval is not to large, as we can see here, we would therefore like to have some data with a higher buoyancy difference. We could do this by increasing the salinity forcing to very extreme heights, however we instead choose to do this by analysing another component of the AMOC relation. As shown in eq. 65 we do also find the vertical diffusivity to have a squared relation with the AMOC instead of the cubic relation found in Bryan (1987). This parameter was also the main value

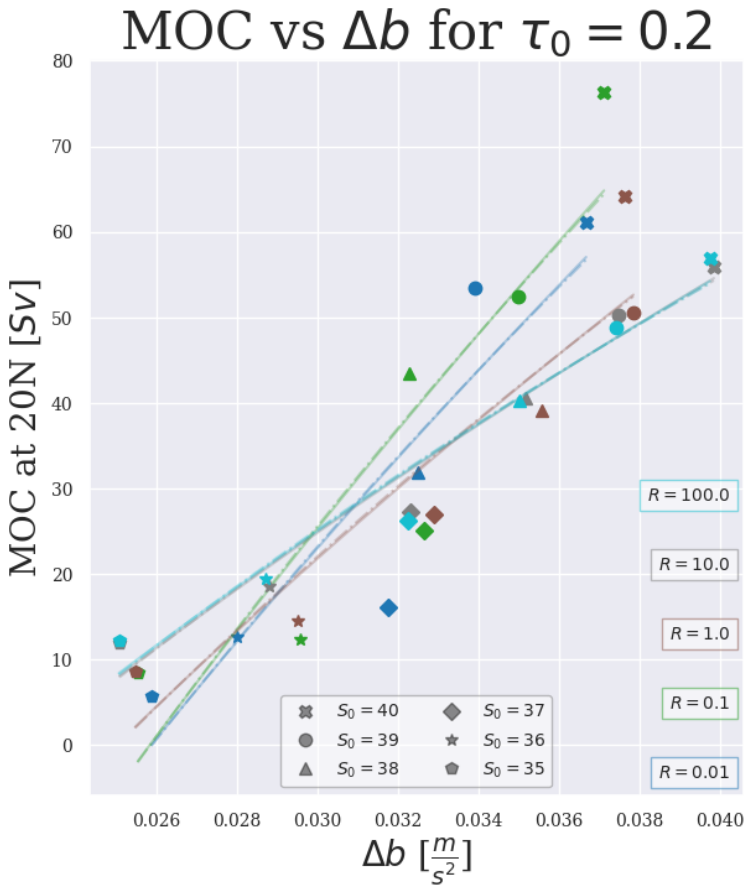

Figure 17: Meridional overturning circulation plotted against the buoyancy forcing for the model runs of w3

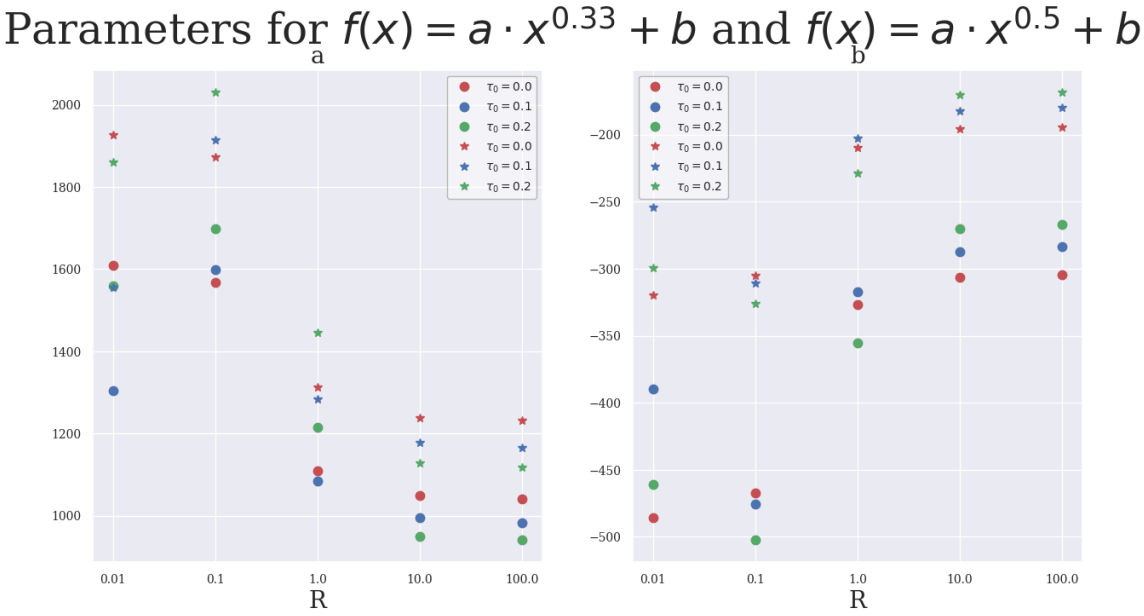

Figure 18: fitting parameters for the two closures. Stars represent the new closure

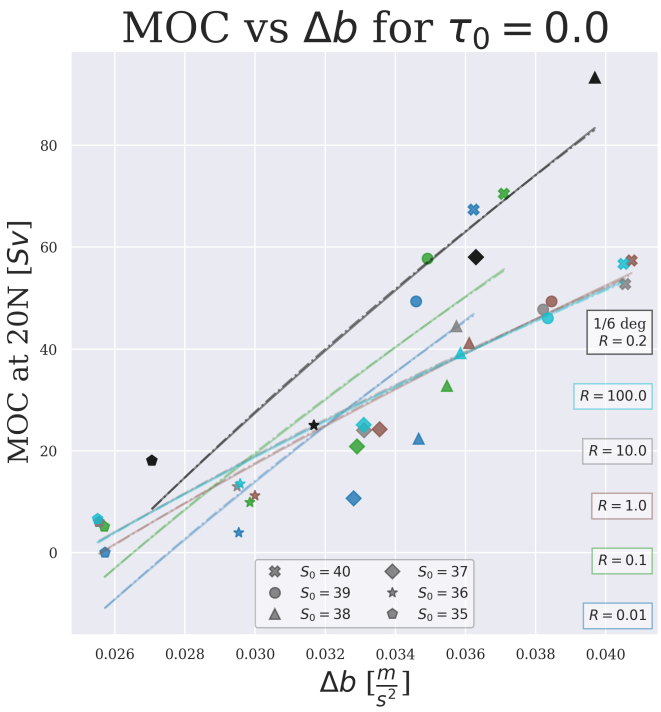

Figure 19: Meridional overturning circulation plotted against the buoyancy forcing for the model runs of w1, including the eddy resolving models

studied in Bryan (1987), and we therefore chose this. As stated we changed the diffusivity in orders of ten to capture a larger interval.

In fig. 20 we have both closures fitted against the data with a logarithmic x-scale to capture the changes. We see that both closures does capture the general trend and even captures the large rise going towards a increase of 100. There is a unexplained dip at around $2 \cdot 10^{-4}$ which is not expected in either closure, which throws both models off, however both models does fit the straightness of the first couple of data points quite well, and both expect the large rise. To quantitative this a bit more we do a simple χ^2 goodness-of-fit test. The cubic and squared functions have a χ^2 value of 1.8 and 2.76 respectively. With three degrees of freedom, they have a χ^2 probability of 0.61 and 0.43 respectively. From this, we can say that both closures do fit the data very well. However due to the dip we can not definitively say that the old closure is better, as it captures this dip slightly better, as this dip is may be a modelling error.

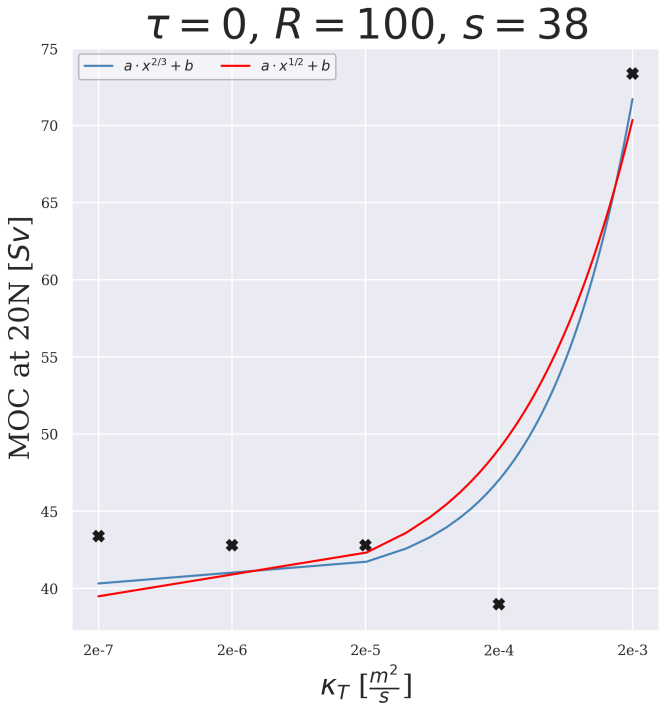

Figure 20: Meridonal overturning circulation plotted against the vertical diffusivity

17

DISCUSSION

We have showed a different way to close the system and get a relation for the AMOC based on buoyancy forcing. This new closure does not use the desperate assumption of switching the gradient in the thermal wind relation as done in Bryan (1987). We instead find a dynamically consistent model relation based on physical properties, and end up with a relation close to that of Bryan (1987). We find a squared relation between the strength of the AMOC and the meridional buoyancy gradient. As shown this relation works just as well as the old closure on this set of data (at least in the interval used). This is due to the two polynomials not being very different over smaller intervals. From this we can also assume the Buoyancy forcing and the southern ocean wind stress to be in a superposition as for the old closure. Now this result in it self would be good, as we show a relation that works just as well as the old, however without the desperate assumption. Nevertheless we also look into how the vertical diffusivity affects the AMOC as this is also a squared relation in our closure and a cubic relation in Bryan (1987). Here we do a large interval of changes in factors of 10 to actually see a difference in the two polynomials. We see that the old closure does capture the data slightly better for this parameter, however this is possible due to the unexplained dip. Both closure do however capture the data well and both have a good χ^2 probability. From this we can argue the new fit to be a good substitute for the old Closure, as it is based on dynamically consistent physics and it captures the model runs to the same level of precision.

Part VI

DISCUSSION

18

SUMMARY

In the first section we looked at the Stommel box model closure found in Bryan (1987) and tested how well the cubic relation found in the paper between the AMOC strength and the meridional buoyancy gradient. We used G&L (2003) as a benchmark and made use of their parameter R. We found the relation to match the model runs for most used R values, however we did see that for very low R values the fit was not great. In G&L (2003) they conclude that for low R values the relation should not hold. We do not believe we can support this claim, as we saw the relation describe the general trend of the data for very low R values and we say it match the data quite well for low R values. We speculated that this might be due to numerical friction however. We therefore also tested against a eddy resolving model with a low R parameter, where we also saw the relation hold. We therefore do not support this claim from G&L (2003). The second point that was made in the paper, was that southern ocean wind stress strengthened the relationship between the AMOC and the buoyancy forcing. We did not see this for higher R values (from around one and up) as the relation was already good with no southern ocean wind stress. We do however see the fit follow the data slightly better for very low R value, but we do not believe we can support the claim based only on this. Nevertheless we did find that the wind stress was in a super position with the buoyancy forcing.

In the second section we looked into the dynamically consistent closure described in B&E

(2011). We found a relation for the AMOC from the density field, by ignoring non linear terms and using the parameterizations described in the paper. We found this closure to work well for coarse resolution models, where we were able to recreate most of the structure and strength of the AMOC. This was however not the case for the eddy resolving models, were the zonal density difference were to strong and negative. We speculate that this is due to the negligence of the non linear terms. We do therefore still believe that the B&E (2011) closure is a good basis for a faster and dynamically consistent zonally averaged model, as the parameterization creates two coupled two dimensional models.

In the last section we formulated a new closure close to that from Bryan (1987). We do however not make the gradient change made in Bryan (1987), and we therefore end up with a dynamically consistent closure. The closure gives a squared relation between the AMOC strength and the buoyancy forcing. We compared this to the data the same way as done in section one, and found the two fits to be identical. To see if there was any different, we also tested the relation between the AMOC and the vertical diffusivity as the relation is the same as for the buoyancy forcing. Here we could use a larger interval. Doing this we found the old closure to fit the data slightly better, however both closures followed the data very well with a good χ^2 probability. We therefore concluded this closure to be a better general choice as it is based in physical properties instead of the desperate gradient change, and the results we found suggested the relation to be as precise.

19

GOALS AND ANSWERS

The main objective of this thesis is to describe the stratification of the abyssal ocean from atmospheric forcings. We quantified this by trying to describe the AMOC as this is a big part of the THC. The AMOC describes the overturning and therefore the stratification in the North Atlantic. The AMOC is density driven with down welling in the arctic region, and up welling in the tropical region. What drives the up welling is not agreed upon. We therefore wanted to test how well the Stommel Box model closure works. In Bryan (1987) a relation for the strength of the AMOC was defined, and we wanted to test how well it works for different horizontal friction. We found that the closure was generally a good description. However we would like to find a different closure for the strength of the AMOC without the assumption that you can change the density gradient in the thermal wind relation from zonally to meridionally. We found a new closure on section three that does not use this change and instead uses physical properties. This means this new closure is dynamically consistent compared to the old. We find this new relation to work just as well for describing the relation between the AMOC strength and the buoyancy gradient. To see a different we also checked the relation between the AMOC strength and the vertical diffusivity. From this we therefore have a dynamically consistent relation that describes the AMOC strength from the atmospheric buoyancy forcing. We also find the windstress to be in a superposition

with the buoyancy forcing. To describe the structure of the AMOC, we find the B&E (2011) closure to be a good choice for coarse resolution models.

20

PROBLEMS

Lastly we would like to point out some of the problems still present. Firstly we will talk about the B&E (2011) closure for the 2.5 dimensional model. We found that this closure can be used to recreate the AMOC from the density field and the zonal velocity field by ignoring the non linearities. Now firstly this is still a prognostic model and need to evolve in time. As can be seen in the appendix we tried solving the closure using the parameterization and ignoring the non linear terms, however the system could not be closed due to scaling of the mass conservation in three dimensions. We also see that this closure only recreates the structure of the AMOC for coarse resolution models and not eddy resolving models. We expect this is due to the non linear terms being neglected. Lastly this closure also need to arbitrary tuning parameters.

Secondly for the new closure and new relation for the AMOC strength, we do still make some assumptions. Firstly the model still uses the empirical Munk's equation, making the closure quasi-empirical and not entirely based on theory. There are other assumption, however we believe these to be founded in physical properties. However we do still see the divergence from this closure for very low R values. This would need to be studied more in depth, and with eddy resolving models to make sure that numerical friction does not affect the R value. Numerical friction is still a worry in our results, even though the eddy resolving models do agree with the results. To be sure one would need to do the very low R value runs in high

resolution as well.

We also see a stranger dip in the vertical diffusivity runs, which we currently can not explain.

Part VII

CONCLUSION

21

CONCLUSION

In this thesis we have outline some of the problems with the current descriptions of the THC. The drive for the tropical up welling is still up for debate and one of the current solutions is the Stommel box model closure and the relationship between the AMOC and the buoyancy forcings as described in Bryan (1987). This model is dynamically inconsistent and another solution based on theory is desirable. However we showed that this Closure does still hold, even for small horizontal frictions, however it does not work great for very small values. we then looked into using the B&E (2011) closure to solve this problem, but did not find a way to close the system. Nevertheless this closure is great for a fast prognostic 2.5 dimensional model of the AMOC, for coarse resolution models. Lastly we looked into a new closure based on the zonal split of the ocean done in B&E (2011). We found that using this, and some other assumptions, one could get a dynamically consistent relationship between the AMOC and the buoyancy forcing. We found this relationship to hold as well as the old one. However when looking at the relationship between the AMOC and the vertical diffusivity, this old closure is slightly better, but the results needs to be taken with reservation due to the dip. We also found the wind stress to be in a superposition with the buoyancy forcing. We therefore conclude that this new closure would be a better choice, as it does not make use of the radical gradient change assumption done in Bryan (1987), and it matches the data just as well for the buoyancy gradient, and in fact better for the vertical diffusivity.

Part VIII

APPENDICES

22

FAILED CLOSURES

We start from the zonally averaged momentum equations defined in equation 27 ans 28 in Brüggemann and Eden:

$$\frac{\partial \bar{u}_\alpha}{\partial t} - f\bar{v}_\alpha = -\frac{1}{\rho_0}\frac{\Delta p_\alpha}{B_\alpha} + \bar{F}^u_\alpha \tag{67}$$

$$\frac{\partial \bar{v}_\alpha}{\partial t} + f\bar{u}_\alpha = -\frac{1}{\rho_0}\frac{\partial \bar{p}_\alpha}{\partial y} + \bar{F}^v_\alpha \tag{68}$$

Where the α subscript can be either b or i, describing the boundary box and interior box respectively. We now firstly assume the geostrophic balance (we also assume no windstress):

$$f\bar{v}_\alpha = \frac{1}{\rho_0}\frac{\Delta p_\alpha}{B_\alpha} \tag{69}$$

$$f\bar{u}_\alpha = -\frac{1}{\rho_0}\frac{\partial \bar{p}_\alpha}{\partial y} \tag{70}$$

We then take the vertical derivative:

$$f\frac{\partial \bar{v}_\alpha}{\partial z} = \frac{1}{\rho_0 B_\alpha}\frac{\partial \Delta p_\alpha}{\partial z} \tag{71}$$

$$f\frac{\partial \bar{u}_\alpha}{\partial z} = -\frac{1}{\rho_0}\frac{\partial}{\partial y}\left(\frac{\partial \bar{p}_\alpha}{\partial z}\right) \tag{72}$$

In eq (72) n we can now simply insert the hydrostatic equation:

$$f\frac{\partial \bar{u}_\alpha}{\partial z} = \frac{g}{\rho_0}\frac{\partial \bar{\rho}_\alpha}{\partial y} \tag{73}$$

For the zonal equation we need to handle each box separately. We start with the boundary box, where the following parameterization is defined in equation 31 in Brüggemann and Eden:

$$\Delta p_b = \gamma_2(\bar{p}_i - \bar{p}_b) \tag{74}$$

Where γ_2 is a tuning parameter. We insert this into the zonal equation above and again use hydrostatic:

$$f\frac{\partial \bar{v}_b}{\partial z} = \frac{\gamma_2}{\rho_0 B_b}(\frac{\partial \bar{p}_i}{\partial z} - \frac{\partial \bar{p}_b}{\partial z}) \tag{75}$$

$$f\frac{\partial \bar{v}_b}{\partial z} = -\frac{g\gamma_2}{\rho_0 B_b}\Delta^x \rho \tag{76}$$

Here $\Delta^x \rho = \bar{\rho}_i - \bar{\rho}_b$ and the x is the remind us of the direction of the difference.

We now go to the interior where we in equation 31 in Brüggemann and Eden have the following parameterization:

$$\Delta p_i = \rho_0 \Delta p_i(y=0) + \rho_0 \gamma_1 \int_0^y f\bar{u}_b dy' \tag{77}$$

Where $\Delta p_i(y=0)$ is the interior pressure difference at the equator, and is defined from the momentum balance at the equator, which is zero in our assumptions. We now insert into our zonal momentum balance:

$$f\frac{\partial \bar{v}_i}{\partial z} = \frac{\gamma_1}{B_i}\frac{\partial}{\partial z}(\int_0^y f\bar{u}_b dy') \tag{78}$$

$$f\frac{\partial \bar{v}_i}{\partial z} = \frac{\gamma_1}{B_i}\int_0^y f\frac{\partial \bar{u}_b}{\partial z} dy' \tag{79}$$

We now have four equations that we can scale:

$$f\frac{\partial \bar{v}_b}{\partial z} = -\frac{g\gamma_2}{\rho_0 B_b}\Delta^x \rho \rightarrow f\frac{V_b}{D} = -\frac{g\gamma_2}{\rho_0 B_b}\Delta^x \rho \tag{80}$$

$$f\frac{\partial \bar{v}_i}{\partial z} = \frac{\gamma_1}{B_i}\int_0^y f\frac{\partial \bar{u}_b}{\partial z} dy' \rightarrow f\frac{V_i}{D} = \frac{\gamma_1}{B_i} f\frac{U_b}{D} L \tag{81}$$

$$f\frac{\partial \bar{u}_b}{\partial z} = \frac{g}{\rho_0}\frac{\partial \bar{\rho}_b}{\partial y} \rightarrow f\frac{U_b}{D} = \frac{g}{\rho_0}\frac{\Delta^y \rho_b}{L} \tag{82}$$

$$f\frac{\partial \bar{u}_i}{\partial z} = \frac{g}{\rho_0}\frac{\partial \bar{\rho}_i}{\partial y} \rightarrow f\frac{U_i}{D} = \frac{g}{\rho_0}\frac{\Delta^y \rho_i}{L} \tag{83}$$

Here D is the depth, L is the meridonal distance, B_b is the zonal width of the boundary, B_i is the zonal with of the interior and $\Delta^y \rho_b$ and $\Delta^y \rho_i$ is the meridonal difference of the density in the boundary and interior respectively.

We now want to eliminate D, and for this we use the density equation described in equation 29 and the continuity equation described in equation 30 in Brüggemann and Eden:

$$\frac{\partial \bar{b}_\alpha}{\partial t} + \frac{\partial \bar{b}_\alpha}{\partial y}\bar{v}_\alpha + \frac{\partial \bar{w}_\alpha}{\partial z}\bar{b}_\alpha = \frac{\partial \kappa_\alpha}{\partial z}\frac{\partial \bar{b}_\alpha}{\partial z} - \varepsilon_\alpha u_\delta \frac{\bar{b}_\alpha}{B_\alpha} \tag{84}$$

$$\varepsilon_\alpha \frac{u_\delta}{B_\alpha} + \frac{\partial \bar{v}_\alpha}{\partial y} + \frac{\partial \bar{w}_\alpha}{\partial z} = 0 \tag{85}$$

Where ε_α is 1 for b and -1 for i, $\bar{b}_\alpha$ is the buoyancy and u_δ is the last parameterization defined as:

$$u_\delta = \gamma_1 \bar{u}_b \tag{86}$$

We now simplify the density equation:

$$\frac{\partial \bar{w}_\alpha}{\partial z}\bar{b}_\alpha = \frac{\partial \kappa_\alpha}{\partial z}\frac{\partial \bar{b}_\alpha}{\partial z} \tag{87}$$

We then scale both equations:

$$\frac{\partial \bar{w}_\alpha}{\partial z}\bar{b}_\alpha = \frac{\partial \kappa_\alpha}{\partial z}\frac{\partial \bar{b}_\alpha}{\partial z} \rightarrow \frac{W_\alpha}{D} b_\alpha = \frac{\kappa_\alpha}{D}\frac{b_\alpha}{D} \tag{88}$$

$$W_\alpha = \frac{\kappa_\alpha}{D} \tag{89}$$

$$\varepsilon_\alpha \frac{u_\delta}{B_\alpha} + \frac{\partial \bar{v}_\alpha}{\partial y} + \frac{\partial \bar{w}_\alpha}{\partial z} = 0 \rightarrow \varepsilon_\alpha \frac{U_\delta}{B_\alpha} + \frac{V_\alpha}{L} + \frac{W_\alpha}{D} = 0 \tag{90}$$

We then merge these two equations and the parameterization. We also decide to look at the boundary box (meaning α will be b) as the parameterization uses the zonal velocity from this box:

$$-\frac{\kappa_b}{D} = \frac{U_\delta D}{B_b} + \frac{V_b D}{L} \tag{91}$$

$$D^2 = -\frac{\kappa_b B_b L}{\gamma_1 U_b L + V_b B_b} \tag{92}$$

We then insert the scaled momentum equations:

$$D^2 = -\frac{\kappa_b B_b L}{\gamma_1(\frac{gD}{\rho_0 f}\frac{\Delta^y \rho_b}{L})L + (-\frac{g\gamma_2 D}{\rho_0 B_b f}\Delta^x \rho)B_b} \tag{93}$$

$$D^3 = \frac{f\rho_0 L B_b \kappa_b}{g(\gamma_2 \Delta^x \rho - \gamma_1 \Delta^y \rho_b)} \tag{94}$$

We now have everything we need, and can find the AMOC, which we define as the meridonal flux:

$$\Phi = DBV \tag{95}$$

We here use equation 10 from Brüggemann and Eden:

$$\Phi = D(B_b \bar{v}_b + B_i \bar{v}_i) \tag{96}$$

We start by inserting our scaled momentum equations:

$$\Phi = D(B_i \frac{\gamma_1 L}{B_i} U_b - B_b \frac{\gamma_2 g D}{f\rho_0 B_b}\Delta^x \rho) \tag{97}$$

$$\Phi = D(\gamma_1 L \frac{gD}{f\rho_0 L}\Delta^y \rho_b - \gamma_2 \frac{gD}{f\rho_0}\Delta^x \rho) \tag{98}$$

$$\Phi = \frac{g}{f\rho_0} D^2(\gamma_1 \Delta^y \rho_b - \gamma_2 \Delta^x \rho) \tag{99}$$

We now lastly insert our equation for D:

$$\Phi = \frac{g}{f\rho_0}(\frac{f\rho_0 L B_b \kappa_b}{g(\gamma_2 \Delta^x \rho - \gamma_1 \Delta^y \rho_b)})^{\frac{2}{3}}(\gamma_1 \Delta^y \rho_b - \gamma_2 \Delta^x \rho) \tag{100}$$

$$\Phi = (\frac{g}{f\rho_0})^{\frac{1}{3}}(L B_b \kappa_b)^{\frac{2}{3}} \frac{(\gamma_1 \Delta^y \rho_b - \gamma_2 \Delta^x \rho)}{(\gamma_2 \Delta^x \rho - \gamma_1 \Delta^y \rho_b)^{\frac{2}{3}}} \tag{101}$$

$$\Phi = -(\frac{g\kappa_b^2 B_b^2 L^2}{f\rho_0})^{\frac{1}{3}}(\gamma_2 \Delta^x \rho - \gamma_1 \Delta^y \rho_b)^{\frac{1}{3}} \tag{102}$$

The problem with this closure is the scaling of the three dimensional mass conservation. The scaling done in this closure does not hold, and we can therefore not close the set of equations from the B&E paper. We have also tried using the Sverdrup relation, however the set could still not be closed

23

FIGURES

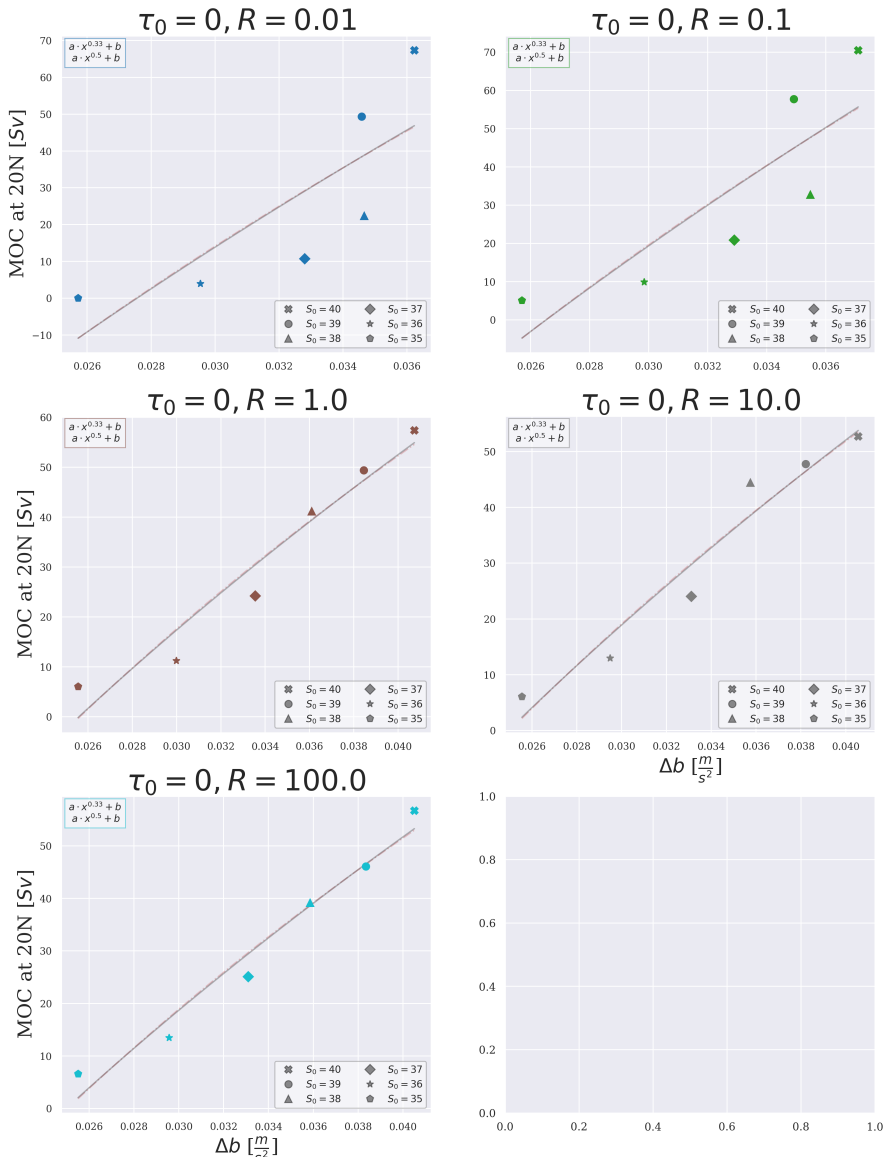

Figure 21: AMOC strength plotted against the buoyancy forcing for the model runs of w1

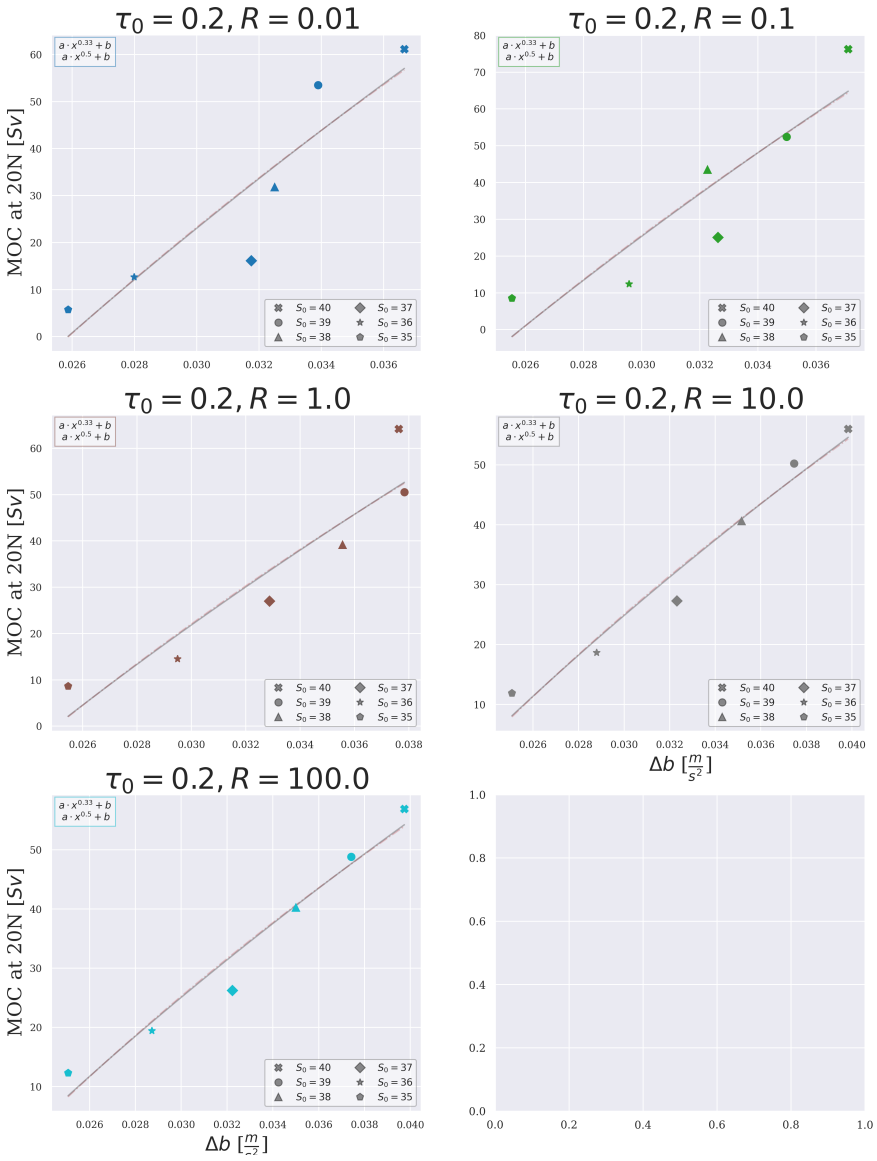

Figure 22: AMOC strength plotted against the buoyancy forcing for the model runs of w2

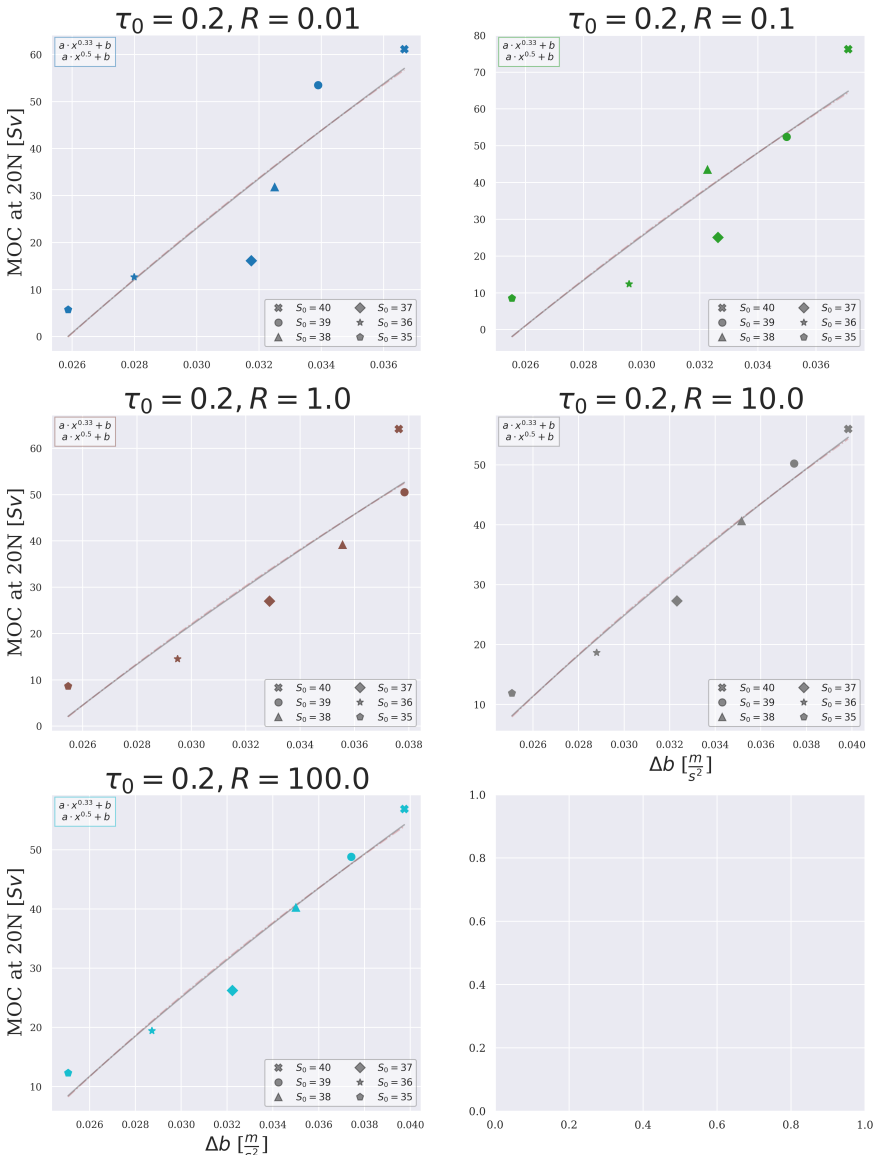

Figure 23: AMOC strength plotted against the buoyancy forcing for the model runs of w3

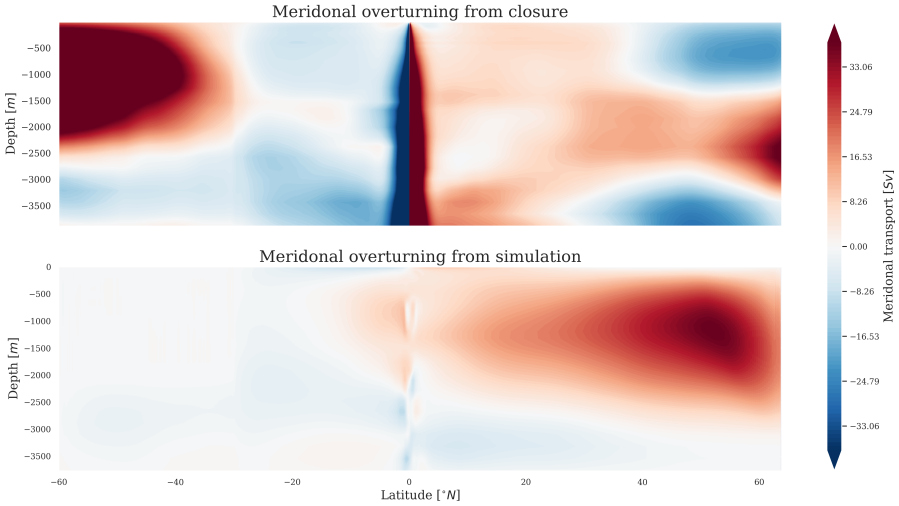

Figure 24: The overturning calculated from the closure and the overturning from VEROS for the 1/6 deg model with no salinity forcing

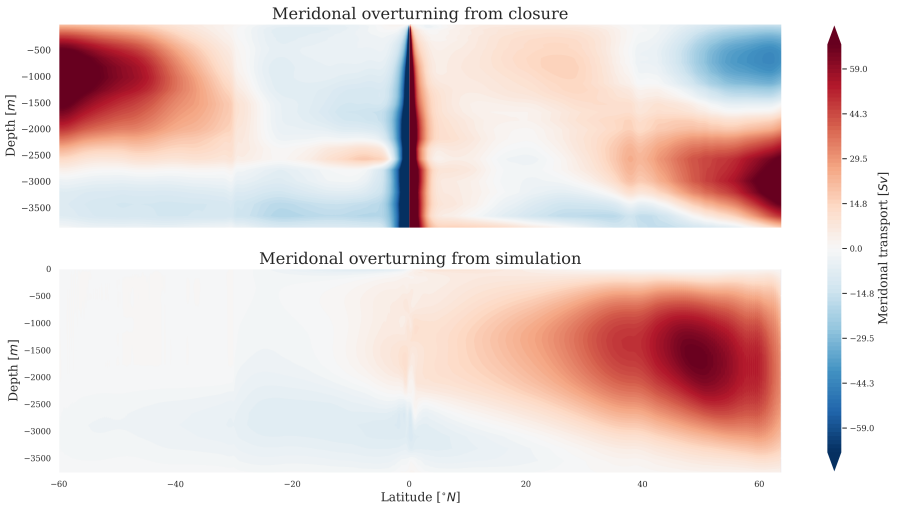

Figure 25: The overturning calculated from the closure and the overturning from VEROS for the 1/6 deg model with 36 salinity forcing

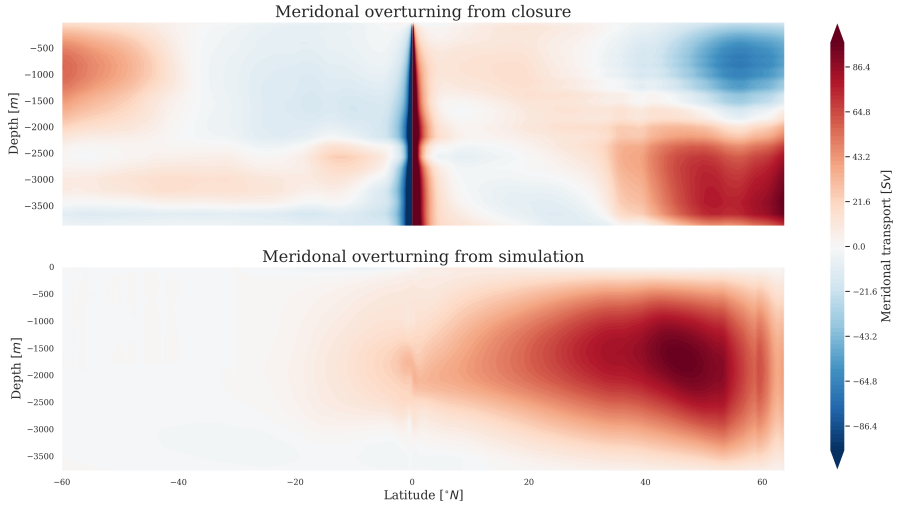

Figure 26: The overturning calculated from the closure and the overturning from VEROS for the 1/6 deg model with 37 salinity forcing

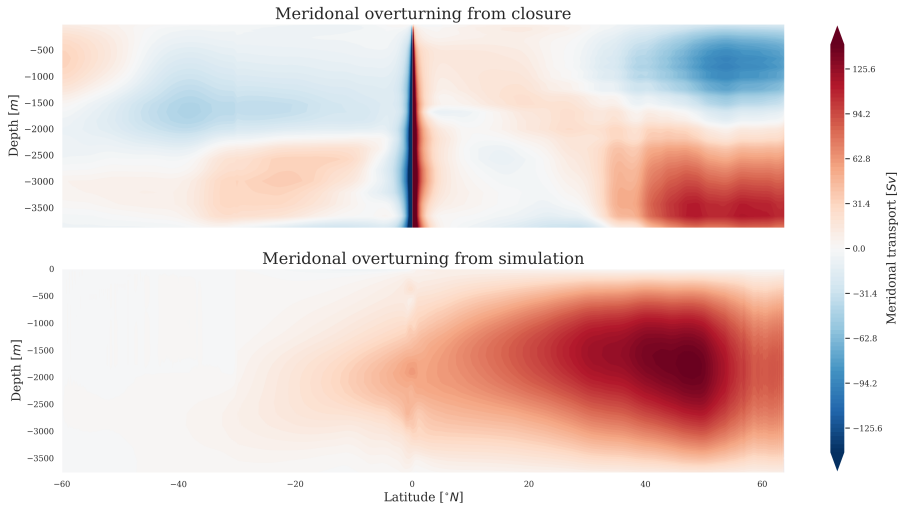

Figure 27: The overturning calculated from the closure and the overturning from VEROS for the 1/6 deg model with 38 salinity forcing

BIBLIOGRAPHY

Andreasen, Laurits S. (2019). "Time scales of the Bipolar seesaw: The role of oceanic cross-hemisphere signals, Southern Ocean eddies and wind changes". MA thesis. University of Copenhagen.

Brüggemann, N., C. Eden, and D. Olbers (2011). "A Dynamically Consistent Closure for Zonally Averaged Ocean Models". In: *J. Phys. Oceanogr.* 41, pp. 2242–2258. DOI: https://doi.org/10.1175/JPO-D-11-021.1.

Bryan, F. (1987). "Parameter Sensitivity of Primitive Equation Ocean General Circulation Models". In: *J. Phys. Oceanogr.* 17, pp. 970–985. DOI: https://doi.org/10.1/1520-0485(1987)017<0970:PSOPEO>2.0.CO;2.

Gaspar, P., Y. Grégoris, and J.-M. Lefevre (1990). "A simple eddy kinetic energy model for simulations of the oceanic vertical mixing: Tests at station Papa and long-term upper ocean study site". In: *J. Geophys. Res.* 95, C9, pp. 16179–16193. DOI: doi:10.1029/JC095iC09p16179.

Greatbatch, R. J. and J. Lu (2003). "Reconciling the Stommel Box Model with the Stommel–Arons Model: A Possible Role for Southern Hemisphere Wind Forcing?" In: *J. Phys. Oceanogr.* 33, pp. 1618–1632. DOI: https://doi.org/10.1175/1520-0485(2003)033<1618:RTSBMW>2.0.CO;2.

Häfner, D. et al. (2018). "Veros v0.1 – a fast and versatile ocean simulator in pure Python". In: *Geosci. Model Dev.* 11, pp. 3299–3312. DOI: https://doi.org/10.5194/gmd-11-3299-2018.

Jochum, M. et al. (2008). "Ocean viscosity and climate". In: *J. Geophys. Res.* 113, p. C06017. DOI: doi:10.1029/2007JC004515.

Munk, W. H. (1986). "Abyssal recipes". In: *Deep Sea Research and Oceanographic Abstracts* 13, 4, pp. 707–730. DOI: https://doi.org/10.1016/0011-7471(66)90602-4.

Stommel, H. (1961). "Thermohaline Convection with Two Stable Regimes of Flow". In: *Tellus* 13, pp. 224–230. DOI: https://doi.org/10.1111/j.2153-3490.1961.tb00079.x.

Stommel, H. and A.B. Arons (1959). "On the abyssal circulation of the world ocean—I. Stationary planetary flow patterns on a sphere". In: *Deep Sea Research (1953)* 6, pp. 140–154. DOI: https://doi.org/10.1016/0146-6313(59)90065-6.

Straub, D.N. (1996). "An inconsistency between two classical models of the ocean buoyancy driven circulation". In: *Tellus A* 48, pp. 477–481. DOI: https://doi.org/10.1034/j.1600-0870.1996.t01-2-00009.x.

Vallis, Geoffrey K. (2017). *Atmospheric and Oceanic Fluid Dynamics, Fundamentals and Large-Scale Circulation*. 2nd. Cambridge University Press. Chap. 21: The Meridional Overturning Circulation and the Antarctic Circumpolar Current. ISBN: 9781107588417.

Vettoretti, G., P. Ditlevsen, and M. et al. Jochum (2022). "Atmospheric CO2 control of spontaneous millennial-scale ice age climate oscillations". In: *Nat. Geosci.* 15, pp. 300–306. DOI: https://doi.org/10.1038/s41561-022-00920-7.